**Stretto di Messina**

Concessionaria per la progettazione, realizzazione e gestione del collegamento stabile tra la Sicilia
e il Continente Organismo di Diritto Pubblico
(Legge n° 1158 del 17 dicembre 1971, modificata dal D.Lgs. n°114 del 24 aprile 2003)

EurolinK

# PONTE SULLO STRETTO DI MESSINA

# PROGETTO DEFINITIVO

## EUROLINK S.C.p.A.

IMPREGILO S.p.A. (MANDATARIA)
SOCIETÀ ITALIANA PER CONDOTTE D'ACQUA S.p.A. (MANDANTE)
COOPERATIVA MURATORI E CEMENTISTI - C.M.C. DI RAVENNA SOC. COOP. A.R.L. (MANDANTE)
SACYR S.A.U. (MANDANTE)
ISHIKAWAJIMA - HARIMA HEAVY INDUSTRIES CO. LTD (MANDANTE)
A.C.I. S.C.P.A. - CONSORZIO STABILE (MANDANTE)

| IL PROGETTISTA | IL CONTRAENTE GENERALE | STRETTO DI MESSINA | STRETTO DI MESSINA |
|---|---|---|---|
| COWI<br>Ing. E.M. Veje<br>Dott. Ing. E. Pagani<br>Ordine Ingegneri Milano<br>n° 15408<br>EurolinK | Project Manager<br>(Ing. P.P. Marcheselli) | Direttore Generale e<br>RUP Validazione<br>(Ing. G. Fiammenghi) | Amministratore Delegato<br>(Dott. P. Ciucci) |

| | | |
|---|---|---|
| *Unità Funzionale* | OPERA DI ATTRAVERSAMENTO | PB0038_F0 |
| *Tipo di sistema* | STUDI DI BASE | |
| *Raggruppamento di opere/attività* | STUDI AERODINAMICO (ANALITICI E SPERIMENTALI) | |
| *Opera - tratto d'opera - parte d'opera* | Basic Studies | |
| *Titolo del documento* | Aerodynamic Calculations, Buffeting | |

CODICE C G 1 0 0 0 P C L D P S B S 3 0 0 0 0 0 0 0 0 0 3 F0

| REV | DATA | DESCRIZIONE | REDATTO | VERIFICATO | APPROVATO |
|---|---|---|---|---|---|
| F0 | 20/06/2011 | EMISSIONE FINALE | SCC/ALN | SAMI | ALN/EYA |
| | | | | | |
| | | | | | |

NOME DEL FILE: PB0038_F0

# INDICE

# 1 Executive summary

## 1.1 Scope

The scope of this report is to analyse the structural response of the Messina Bridge structure to gusty wind (buffeting) analysed using two different methods:

1) Frequency domain analysis following the quasi-steady approach (Dynwind).

2) Time domain analysis applying synthetic simulated wind series supplied by SdM.

## 1.2 Conclusion

The result of the analyses show that the frequency domain and time domain approach to analyse the dynamic wind response of the Messina Bridge give similar results.

The responses from the time history analyses show that the dominant modes of vibration are the 1$^{st}$ and 2$^{nd}$ transversal mode of the deck, i.e. approx 30sec and 20sec vibration period.

The response from ULS is slightly higher than the response found from the dynamic wind analysis in short intervals, which can be explained by the contents of the time series.

The dynamic wind analyses carried out during design does not take admittance into account, which from the results is seen to be a conservative approach.

It is proposed that further comparative studies between buffeting calculations and wind tunnel test are carried out during the Progetto Esecutivo phase once the results of the planned full bridge model test becomes available.

# 2 Aerodynamic input

## 2.1 Wind load coefficients

### 2.1.1 Girder

Wind load coefficients for the bridge girder without traffic and in beam wind (perpendicular to the girder) are adopted from the wind tunnel tests carried out at FORCE in turbulent wind as these tests provide the most conservative values, [1], [6] as shown in Figure 2.1. Values for traffic and skew wind attack angles (yaw) are adopted from the tests carried out at BLWTL, [4].

Drag, lift and moment coefficients are defined as follows:

Drag, Lift: $$C_{D,L} = \frac{D,L}{½\rho U^2 B}$$

Moment: $$C_M = \frac{M}{½\rho U^2 B^2}$$

where B = 60.4 m is the total width of the girder and U is the mean wind speed.
Wind perpendicular to the girder (beam wind) is 0°.

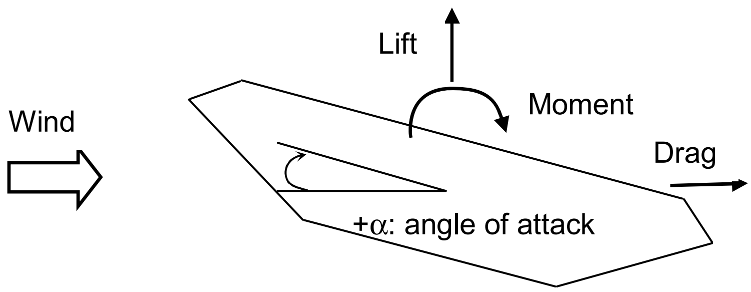

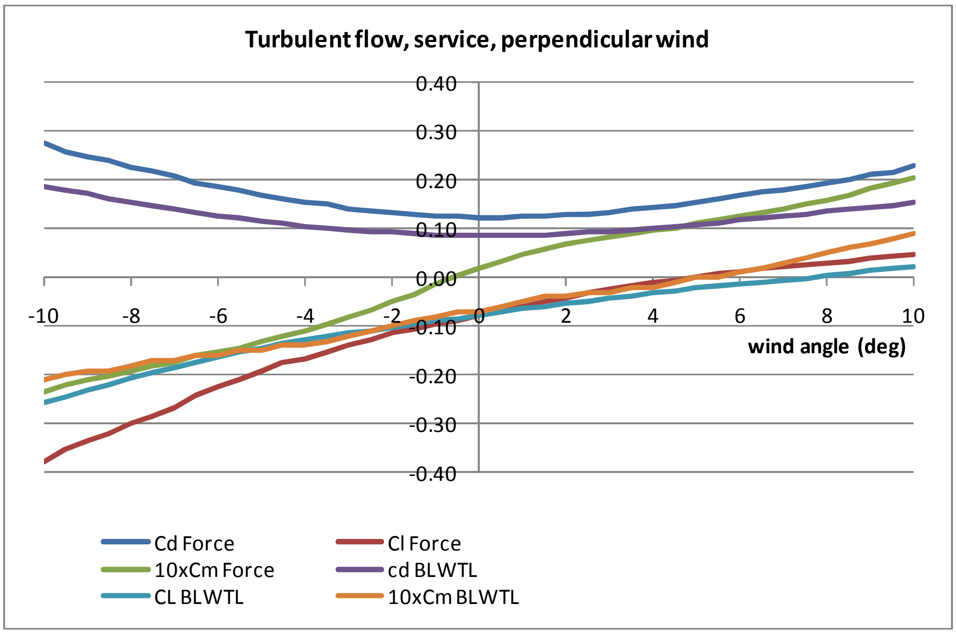


*Figure 2.1 Static wind load coefficients fro the two parallel tests (sub-tests D3 and D4), no traffic. Turbulent flow, perpendicular wind.*

*Table 2.1 Wind load coefficients for the girder, Messina Strait Bridge, in-service (without traffic). B = 60.4m. Horizontal wind.*

| yaw angle | $C_D$ | $dC_D/d\alpha$ | $C_L$ | $dC_L/d\alpha$ | $C_M$ | $dC_M/d\alpha$ |
|---|---|---|---|---|---|---|
| -10 | 0.275 | | -0.377 | | -0.024 | |
| -9.5 | 0.258 | | -0.352 | | -0.022 | |
| -9 | 0.247 | | -0.334 | | -0.021 | |
| -8.5 | 0.240 | | -0.321 | | -0.02 | |
| -8 | 0.227 | | -0.299 | | -0.019 | |
| -7.5 | 0.219 | | -0.284 | | -0.018 | |
| -7 | 0.209 | | -0.266 | | -0.017 | |
| -6.5 | 0.195 | | -0.242 | | -0.016 | |
| -6 | 0.187 | | -0.225 | | -0.015 | |
| -5.5 | 0.179 | | -0.210 | | -0.014 | |
| -5 | 0.170 | | -0.192 | | -0.013 | |
| -4.5 | 0.160 | | -0.175 | | -0.012 | |
| -4 | 0.156 | | -0.165 | | -0.011 | |
| -3.5 | 0.149 | | -0.152 | | -0.010 | |
| -3 | 0.141 | | -0.138 | | -0.008 | |
| -2.5 | 0.137 | | -0.126 | | -0.007 | |
| -2 | 0.132 | | -0.114 | | -0.005 | |
| -1.5 | 0.129 | | -0.106 | | -0.003 | |
| -1 | 0.127 | | -0.096 | | -0.001 | |
| -0.5 | 0.126 | | -0.088 | | 0.000 | |
| **0** | **0.122** | **-0.04** | **-0.077** | **1.06** | **0.002** | **0.18** |
| 0.5 | 0.122 | | -0.068 | | 0.003 | |
| 1 | 0.125 | | -0.059 | | 0.005 | |
| 1.5 | 0.124 | | -0.050 | | 0.006 | |
| 2 | 0.129 | | -0.042 | | 0.007 | |
| 2.5 | 0.131 | | -0.033 | | 0.008 | |
| 3 | 0.134 | | -0.026 | | 0.008 | |
| 3.5 | 0.139 | | -0.018 | | 0.009 | |
| 4 | 0.144 | | -0.011 | | 0.010 | |
| 4.5 | 0.148 | | -0.005 | | 0.010 | |
| 5 | 0.156 | | 0.002 | | 0.011 | |
| 5.5 | 0.163 | | 0.007 | | 0.012 | |
| 6 | 0.169 | | 0.013 | | 0.013 | |
| 6.5 | 0.176 | | 0.017 | | 0.013 | |
| 7 | 0.180 | | 0.021 | | 0.014 | |
| 7.5 | 0.188 | | 0.026 | | 0.015 | |
| 8 | 0.194 | | 0.029 | | 0.016 | |
| 8.5 | 0.201 | | 0.034 | | 0.017 | |
| 9 | 0.211 | | 0.039 | | 0.018 | |
| 9.5 | 0.217 | | 0.043 | | 0.019 | |
| 10 | 0.228 | | 0.047 | | 0.020 | |

*Table 2.2 Wind load coefficients for the girder, Messina Strait Bridge, construction. B = 60.4m. Horizontal wind.*

| yaw angle | $C_D$ | $dC_D/d\alpha$ | $C_L$ | $dC_L/d\alpha$ | $C_M$ | $dC_M/d\alpha$ |
|---|---|---|---|---|---|---|
| -10 | 0.143 | | -0.570 | | -0.040 | |
| -9.5 | 0.133 | | -0.541 | | -0.038 | |
| -9 | 0.126 | | -0.525 | | -0.037 | |
| -8.5 | 0.119 | | -0.504 | | -0.036 | |
| -8 | 0.113 | | -0.486 | | -0.035 | |
| -7.5 | 0.106 | | -0.465 | | -0.033 | |
| -7 | 0.099 | | -0.440 | | -0.032 | |
| -6.5 | 0.093 | | -0.422 | | -0.031 | |
| -6 | 0.087 | | -0.400 | | -0.029 | |
| -5.5 | 0.082 | | -0.382 | | -0.028 | |
| -5 | 0.076 | | -0.359 | | -0.026 | |
| -4.5 | 0.071 | | -0.335 | | -0.023 | |
| -4 | 0.067 | | -0.311 | | -0.021 | |
| -3.5 | 0.063 | | -0.289 | | -0.019 | |
| -3 | 0.058 | | -0.263 | | -0.017 | |
| -2.5 | 0.055 | | -0.237 | | -0.014 | |
| -2 | 0.052 | | -0.21 | | -0.011 | |
| -1.5 | 0.051 | | -0.186 | | -0.009 | |
| -1 | 0.049 | | -0.16 | | -0.006 | |
| -0.5 | 0.049 | | -0.138 | | -0.004 | |
| **0** | **0.049** | **0.06** | **-0.114** | **2.62** | **-0.001** | **0.32** |
| 0.5 | 0.050 | | -0.088 | | 0.003 | |
| 1 | 0.051 | | -0.068 | | 0.005 | |
| 1.5 | 0.053 | | -0.046 | | 0.008 | |
| 2 | 0.056 | | -0.027 | | 0.011 | |
| 2.5 | 0.059 | | -0.008 | | 0.013 | |
| 3 | 0.062 | | 0.011 | | 0.015 | |
| 3.5 | 0.066 | | 0.028 | | 0.017 | |
| 4 | 0.069 | | 0.043 | | 0.019 | |
| 4.5 | 0.076 | | 0.062 | | 0.021 | |
| 5 | 0.081 | | 0.079 | | 0.022 | |
| 5.5 | 0.087 | | 0.094 | | 0.023 | |
| 6 | 0.092 | | 0.106 | | 0.024 | |
| 6.5 | 0.097 | | 0.119 | | 0.024 | |
| 7 | 0.104 | | 0.134 | | 0.024 | |
| 7.5 | 0.111 | | 0.147 | | 0.024 | |
| 8 | 0.115 | | 0.157 | | 0.024 | |
| 8.5 | 0.122 | | 0.169 | | 0.023 | |
| 9 | 0.127 | | 0.178 | | 0.023 | |
| 9.5 | 0.136 | | 0.192 | | 0.023 | |
| 10 | 0.139 | | 0.196 | | 0.023 | |

### 2.1.2 Tower

Drag and lift coefficients are given in the following format (wind coordinate system):

$$C_D = \frac{D}{1/2\rho U^2 B} \qquad C_L = \frac{L}{1/2\rho U^2 B}$$

where D,L = aerodynamic drag/lift force per unit length of girder, $1/2\rho U^2$ = dynamic head of the wind, B = characteristic dimension of the structure (here **B = 20 m** in all cases).

Wind load coefficients for the tower legs are adopted from the wind tunnel tests carried out at BMT, [2]. The measured values correspond to turbulent flow as they were generally the highest and thus most conservative. An angle of 0° correspond to wind across the bridge, 90° corresponds to wind along the bridge.

The wind tunnel tests at BMT covered the case with both tower legs and the case with only a single leg. From this, the values for the upwind leg has been approximated as the measured single leg values and values for the downwind leg then found by subtracting the values for the upwind leg from the measured total.

*Table 2.3 Wind load coefficients for the tower, Messina Strait Bridge. B = 20m.*

| | Total | | Upwind leg | | Downwind leg | |
|---|---|---|---|---|---|---|
| Angle (deg) | $C_D$ | $C_L$ | $C_D$ | $C_L$ | $C_D$ | $C_L$ |
| **0.0** | **1.8** | **0.0** | **1.8** | **0.0** | **0.0** | **0.0** |
| 5.0 | 1.7 | 0.0 | 1.7 | 0.2 | 0.0 | -0.2 |
| 10.0 | 1.6 | 0.1 | 1.6 | 0.3 | 0.0 | -0.3 |
| 15.0 | 1.8 | 0.3 | 1.4 | 0.5 | 0.4 | -0.2 |
| 20.0 | 1.9 | 0.3 | 1.4 | 0.5 | 0.5 | -0.2 |
| 25.0 | 2.0 | 0.3 | 1.4 | 0.4 | 0.6 | -0.1 |
| 30.0 | 2.0 | 0.4 | 1.3 | 0.4 | 0.7 | -0.1 |
| 35.0 | 1.9 | 0.3 | 1.2 | 0.4 | 0.7 | -0.1 |
| 40.0 | 1.9 | 0.3 | 1.1 | 0.3 | 0.8 | 0.0 |
| **45.0** | **1.7** | **0.2** | **1.0** | **0.3** | **0.7** | **-0.1** |
| 50.0 | 1.5 | 0.1 | 0.8 | 0.2 | 0.7 | -0.1 |
| 55.0 | 1.1 | 0.0 | 0.6 | 0.1 | 0.5 | -0.1 |
| 60.0 | 0.8 | 0.2 | 0.4 | 0.3 | 0.4 | -0.1 |
| 65.0 | 0.7 | 0.0 | 0.4 | 0.1 | 0.3 | -0.1 |
| 70.0 | 0.7 | 0.5 | 0.3 | 0.0 | 0.4 | 0.5 |
| 75.0 | 0.4 | 0.5 | 0.3 | 0.3 | 0.3 | 0.1 |
| 80.0 | 0.5 | 0.9 | 0.2 | 0.5 | 0.3 | 0.4 |
| 85.0 | 0.6 | 0.6 | 0.3 | 0.3 | 0.3 | 0.3 |
| **90.0** | **0.6** | **0.0** | **0.3** | **0.0** | **0.3** | **0.0** |

For the buffeting computations the tower legs are modelled as individual elements using the wind load coefficients given in Table 2.3.

Figure 2.2 shows the DVMFLOW cross section for the tower cross beam. The width of the cross beam is 4 m, and the height is 17.74 m. The drag coefficient for the cross beam is found to be

$$C_{D,\ cross\ beam} = 2.1$$

normalised with B = 17.74 m.

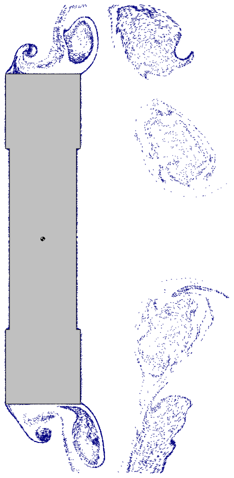

*Figure 2.2 Cross beam cross section. Width = 4 m, Height = 17.74 m.*

### 2.1.3 Hanger cables

The drag coefficient for the individual hanger cables is taken as:

$C_D = 0.8$

The drag coefficient is normalized by hanger diameter d.

### 2.1.4 Main Cables

The drag coefficient for the main cables are adopted from the high Re wind tunnel tests, [3], and taken as:

$C_D = 0.5$ for the upwind cable and $C_D = -0.1$ for the downwind cable.

The drag coefficients are normalized by the actual main cable diameter.

Possible lift effects on the twinned main cables were neglected in the computations of mean wind an buffeting responses.

## 2.2 Aerodynamic damping and stiffness reduction

### 2.2.1 Frequency-domain (Dynwind)

Aerodynamic derivatives in smooth flow adopted from the wind tunnel tests at FORCE, [1], [6], are used to calculate the modal aerodynamic damping and stiffness reductions in the frequency-domain buffeting calculations. In two dimensions, the procedure is illustrated below. The aerodynamic derivatives defined according to Scanlan are:

$$L = \frac{1}{2}\rho U^2 (2B)\left( KH_1^*(K)\frac{\dot{z}}{U} + KH_2^*(K)\frac{B\dot{\alpha}}{U} + K^2 H_3^*(K)\alpha + K^2 H_4^*(K)\frac{z}{B} \right)$$

$$M = \frac{1}{2}\rho U^2 (2B^2)\left( KA_1^*(K)\frac{\dot{z}}{U} + KA_2^*(K)\frac{B\dot{\alpha}}{U} + K^2 A_3^*(K)\alpha + K^2 A_4^*(K)\frac{z}{B} \right)$$

where K = ωB/U, L is lift force and M is moment. The frequency domain approach does not include non-linear effects due to changes in the aerodynamic derivatives as function of angle of attack.

The modal aerodynamic damping and stiffness reductions are evaluated as:

$$\zeta_{aero} = -\frac{\rho B^4}{2I_g}\left\{ H_1^* \int_{girder} (z(s))^2 ds + H_2^* \int_{girder} z(s)\alpha(s)ds + A_1^* \int_{girder} z(s)\alpha(s)ds + A_2^* \int_{girder} (\alpha(s))^2 ds \right\}$$

$$k_{aero} = -\rho\omega^2 B^4 \left\{ H_3^* \int_{girder} z(s)\alpha(s)ds + H_4^* \int_{girder} (z(s))^2 ds + A_3^* \int_{girder} (\alpha(s))^2 ds + A_4^* \int_{girder} z(s)\alpha(s)ds \right\}$$

where

$$I_g = \int_{girder} \left(m(s)\left(z(s)\right)^2 B^2 + I(s)(\alpha(s))^2\right) ds$$

and m(s) og I(s) are mass and mass moment of inertia of the girder, z(s) is the vertical deflection and α(s) is the torsion. ρ is the air density.

*Table 2.4 Aerodynamic derivatives, interpolated from Force values for smooth flow.*

| U/(f*B) | H1 | H2 | H3 | H4 | H5 | H6 |
|---|---|---|---|---|---|---|
| **0.45** | -0.4282 | 0.011612 | -0.07869 | 0.814879 | 0.013992 | 0.101274 |
| **0.5** | -0.46903 | 0.004891 | -0.08259 | 0.808011 | 0.003503 | 0.079459 |
| **0.6** | -0.50003 | -0.00279 | -0.06959 | 0.811132 | -0.03016 | 0.079984 |
| **0.7** | -0.54602 | -0.00381 | -0.06912 | 0.843087 | -0.06512 | 0.112661 |
| **2** | -0.70016 | -0.06469 | -0.25717 | 1.059635 | 0.007355 | 0.134754 |
| **3** | -0.83462 | -0.22768 | -0.48667 | 1.306281 | -0.03201 | 0.112672 |
| **5** | -0.8988 | -0.6401 | -0.87591 | 1.655117 | -0.09211 | 0.113072 |
| **7** | -0.80324 | -1.00357 | -1.09127 | 1.508972 | -0.11402 | 0.122825 |
| **9** | -0.72394 | -1.26139 | -1.27394 | 1.146462 | -0.12993 | 0.12604 |
| **11** | -0.70334 | -1.50619 | -1.51002 | 0.909136 | -0.1474 | 0.131685 |
| **13** | -0.73221 | -1.76191 | -1.82137 | 0.787185 | -0.17014 | 0.13301 |
| **15** | -0.77333 | -2.01768 | -2.20408 | 0.6935 | -0.19902 | 0.143008 |
| **16** | -0.7934 | -2.14192 | -2.42002 | 0.668138 | -0.2106 | 0.153756 |
| **18** | -0.83547 | -2.38629 | -2.86964 | 0.677748 | -0.21695 | 0.145615 |
| **21** | -0.92625 | -2.78456 | -3.68644 | 0.611241 | -0.25849 | 0.112259 |
| **23** | -0.98944 | -3.04953 | -4.27723 | 0.567055 | -0.29278 | 0.13417 |
| **25** | -1.06482 | -3.32346 | -4.94799 | 0.557381 | -0.31637 | 0.151066 |
| **27** | -1.10498 | -3.604 | -5.66135 | 0.544372 | -0.3319 | 0.12829 |
| **30** | -1.20233 | -3.9857 | -6.85201 | 0.481526 | -0.37618 | 0.242037 |

| U/(f*B) | A1 | A2 | A3 | A4 | A5 | A6 |
|---|---|---|---|---|---|---|
| **0.45** | 0.009374 | -0.03449 | 0.054619 | -0.01985 | -0.00247 | -0.00202 |
| **0.5** | 0.006001 | -0.03495 | 0.054872 | -0.02335 | -0.0048 | -0.00192 |
| **0.6** | 0.002196 | -0.0348 | 0.056577 | -0.02349 | -0.00648 | 0.003605 |
| **0.7** | -0.00115 | -0.03556 | 0.056994 | -0.02191 | -0.00533 | 0.011813 |
| **2** | 0.030244 | -0.06919 | 0.080191 | -0.02246 | 0.014133 | 0.001372 |
| **3** | 0.025819 | -0.07712 | 0.084425 | -0.00575 | 0.008924 | -0.00721 |
| **5** | 0.06005 | -0.12074 | 0.109307 | 0.037014 | -0.00022 | -0.0122 |
| **7** | 0.121676 | -0.17057 | 0.174736 | 0.051213 | -0.00318 | -0.01331 |
| **9** | 0.16247 | -0.19976 | 0.25822 | 0.051361 | -0.00357 | -0.01391 |
| **11** | 0.193171 | -0.22463 | 0.363593 | 0.050841 | -0.00518 | -0.01031 |
| **13** | 0.224336 | -0.25187 | 0.495164 | 0.053426 | -0.00907 | -0.00492 |
| **15** | 0.258831 | -0.2755 | 0.649293 | 0.051509 | -0.00632 | -0.00705 |
| **16** | 0.277516 | -0.28757 | 0.735984 | 0.049727 | -0.00416 | -0.00827 |
| **18** | 0.316266 | -0.32142 | 0.920364 | 0.057007 | -0.00719 | -0.00131 |
| **21** | 0.358203 | -0.36979 | 1.240305 | 0.066654 | -0.00899 | -0.00845 |
| **23** | 0.388353 | -0.39917 | 1.481806 | 0.067338 | -0.01504 | -0.00427 |
| **25** | 0.426426 | -0.42737 | 1.743737 | 0.069777 | -0.00947 | 0.001386 |
| **27** | 0.462584 | -0.45585 | 2.029322 | 0.080081 | -0.00086 | -0.0285 |
| **30** | 0.509372 | -0.51488 | 2.508455 | 0.095989 | -0.03817 | -0.00192 |

| U/(f*B) | P1 | P2 | P3 | P4 | P5 | P6 |
|---|---|---|---|---|---|---|
| **0.45** | -0.13535 | 0.002127 | 0.050554 | 0.823824 | 0.046505 | -0.01732 |
| **0.5** | -0.12641 | 0.002603 | 0.049388 | 0.831407 | 0.051633 | -0.01768 |
| **0.6** | -0.12311 | 0.000938 | 0.047275 | 0.831954 | 0.056128 | -0.02002 |
| **0.7** | -0.13093 | 0.000713 | 0.047568 | 0.822568 | 0.061085 | -0.02519 |
| **2** | -0.16784 | 0.024306 | 0.058636 | 0.867393 | 0.049562 | -0.061 |
| **3** | -0.18134 | 0.045688 | 0.06574 | 0.882554 | 0.050022 | -0.09074 |
| **5** | -0.20969 | 0.102159 | 0.076014 | 0.890366 | 0.036296 | -0.14124 |
| **7** | -0.22986 | 0.157697 | 0.098033 | 0.875486 | 0.019572 | -0.1529 |
| **9** | -0.23911 | 0.199285 | 0.160983 | 0.852947 | 0.00711 | -0.14845 |
| **11** | -0.24658 | 0.236086 | 0.25417 | 0.842272 | -0.00277 | -0.14311 |
| **13** | -0.26828 | 0.272089 | 0.361473 | 0.838901 | -0.01843 | -0.14173 |
| **15** | -0.28132 | 0.310049 | 0.494462 | 0.845005 | -0.02821 | -0.15684 |
| **16** | -0.28748 | 0.332175 | 0.57393 | 0.858282 | -0.02382 | -0.16163 |
| **18** | -0.33904 | 0.367444 | 0.728983 | 0.851634 | -0.00975 | -0.14716 |
| **21** | -0.36835 | 0.426754 | 0.994252 | 0.86528 | -0.0191 | -0.14002 |
| **23** | -0.40306 | 0.47992 | 1.199811 | 0.847404 | -0.00537 | -0.15678 |
| **25** | -0.44259 | 0.517228 | 1.4281 | 0.889926 | -0.00763 | -0.17754 |
| **27** | -0.40867 | 0.58427 | 1.685498 | 0.837878 | -0.02139 | -0.19591 |
| **30** | -0.50507 | 0.653727 | 2.095766 | 0.797668 | -0.05697 | -0.27566 |

### 2.2.2 Time domain (time history)

The wind loading in horizontal, vertical and torsion is modelled simply by squaring the instantaneous wind speed, multiplying it by ½ρ, the relevant characteristic dimensions and the relevant wind load coefficient obtained at the instantaneous inflow angle. Thus linearization of the aerodynamic load coefficients is not implied. The instantaneous wind forces acting on a section various bridge components are thus modelled as:

$$F_D = \frac{1}{2} \cdot \rho \cdot V^2 \cdot C_D(\alpha) \cdot B \cdot \varDelta$$

$$F_L = \frac{1}{2} \cdot \rho \cdot V^2 \cdot C_L(\alpha) \cdot B \cdot \varDelta$$

$$F_M = \frac{1}{2} \cdot \rho \cdot V^2 \cdot C_M(\alpha) \cdot B^2 \cdot \varDelta$$

Where α is instantaneous wind inflow angle and $\varDelta$ is the separation between adjacent nodes in which the wind loading is imposed. The instantaneous wind speed V and angle of attack α are obtained as:

$$V = \sqrt{(U + u - \dot{x})^2 + (w - \dot{z})^2}$$

$$\alpha = \theta + tan^{-1} \frac{w - \dot{z}}{U + u - \dot{x}}$$

Where U+u is the instantaneous horizontal wind speed, w is the instantaneous vertical wind speed and $\dot{x}$, $\dot{z}$ are the instantaneous horizontal and vertical velocities of the structural cross section and θ is the instantaneous corss section angle of rotation.

## 2.3 Aerodynamic admittance

The following admittance functions are used in the frequency-domain analyses.

Adopted from the wind tunnel tests carried out at FORCE:

$$\mathrm{AL}(f^*)_{\mathrm{FORCE}} = \frac{1.5 \cdot f^{*2.5}}{(0.18 - f^*)^2 + 0.09^2} + \frac{0.50}{1 + 2\pi^2 \cdot f^*}$$

$$\mathrm{AD}(f^*)_{\mathrm{FORCE}} = \frac{2.0 \cdot f^{*1.5}}{(0.20 - f^*)^2 + 0.70^2} + \frac{0.25}{1 + 2\pi^2 \cdot f^*}$$

$$\mathrm{AM}(f^*)_{\mathrm{FORCE}} = \frac{1.9 \cdot f^{*1.8}}{(0.50 - f^*)^2 + 0.18^2} + \frac{0.05}{1 + 2\pi^2 \cdot f^*}$$

$$f^* = \frac{f \cdot B}{U}$$

Adopted from the wind tunnel tests carried out at BLWTL:

$$\mathrm{AL}(f^*)_{\mathrm{BLWTL}} = \frac{2.9 \cdot f^{*1.2}}{(-0.22 - f^*)^2 + 0.18^2} + \frac{0.70}{1 + 2\pi^2 \cdot f^*}$$

$$\mathrm{AD}(f^*)_{\mathrm{BLWTL}} = \frac{0.45}{1 + 0.05\pi^2 \cdot f^*}$$

$$\mathrm{AM}(f^*)_{\mathrm{BLWTL}} = \frac{1.95 \cdot f^{*1.18}}{(-0.15 - f^*)^2 + 0.18^2} + \frac{1}{1 + 2\pi^2 \cdot f^*}$$

$$f^* = \frac{f \cdot B}{U}$$

The above expressions are shown in graphical form in Figure 2.3 and Figure 2.4.

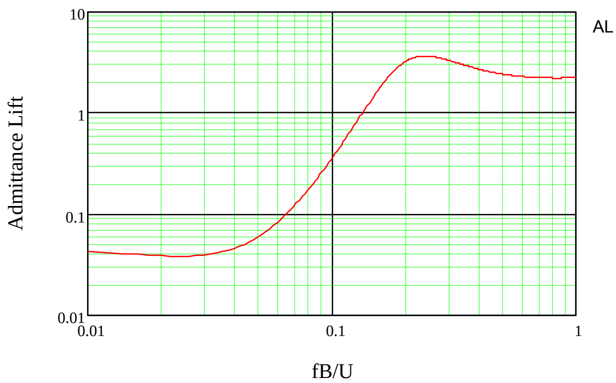


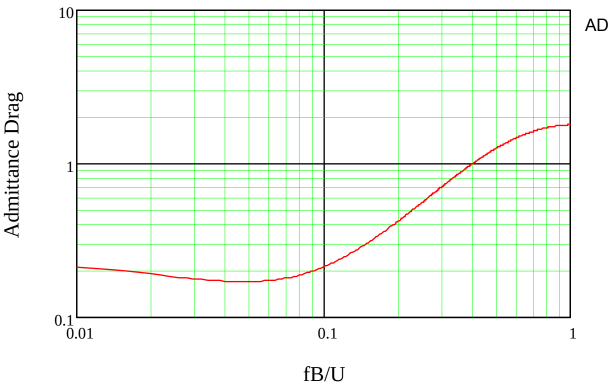

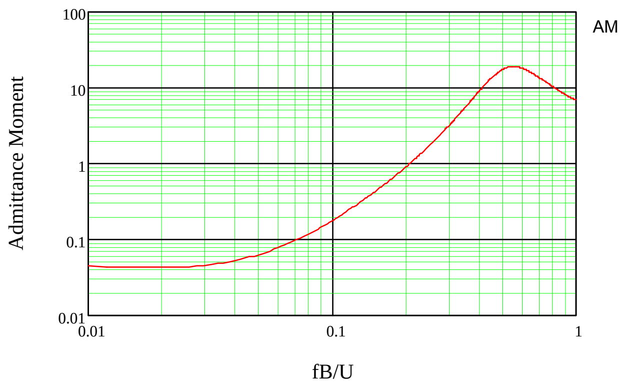


*Figure 2.3 Aerodynamic admittances fitted to FORCE measurements.*

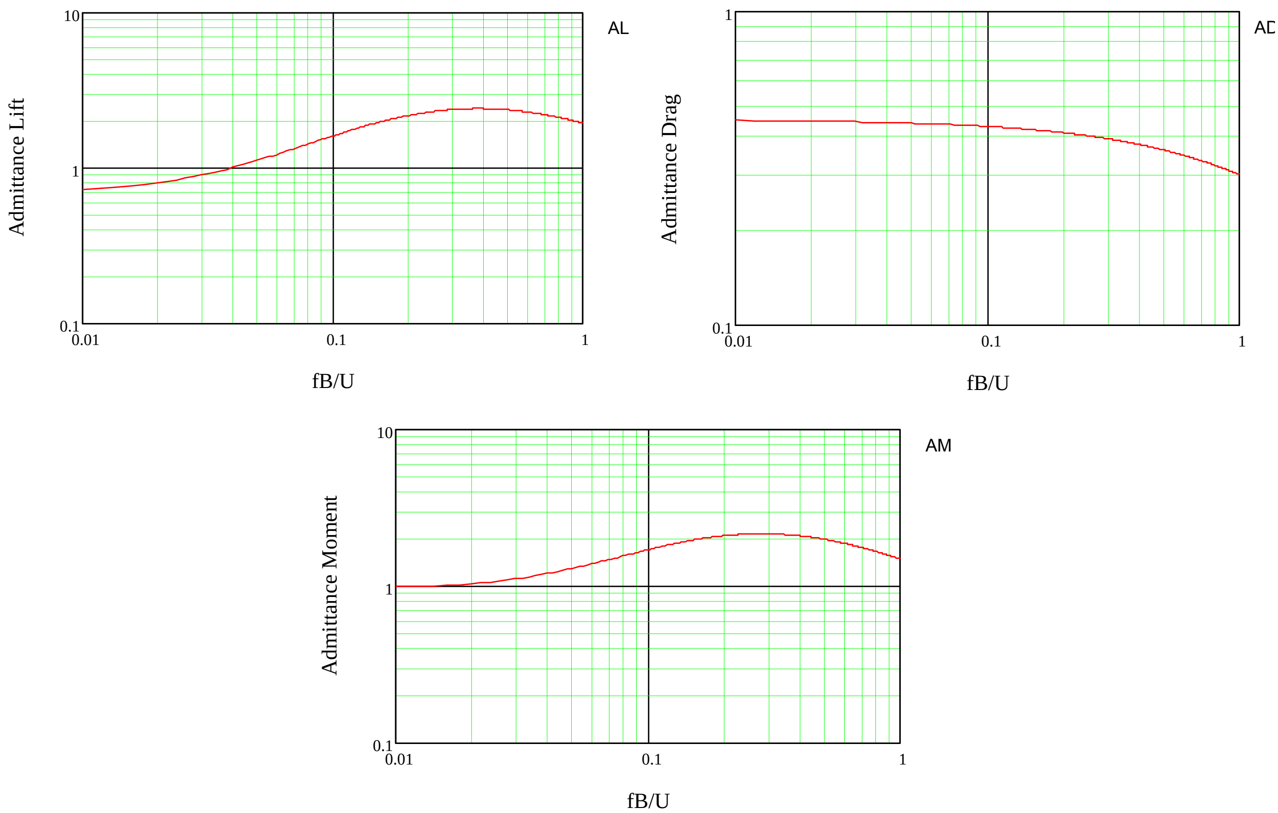


*Figure 2.4 Aerodynamic admittances fitted to BLWTL measurements.*

# 3 Buffeting analyses

## 3.1 Frequency-domain (Dynwind)

In general a wind load due to natural turbulent wind can be considered as the sum of a static mean wind and a stochastic fluctuating wind load, the latter referred to as buffeting load. The response of the structure can similarly be divided into a response to mean wind (static response) and a response to buffeting wind (dynamic response).

The buffeting response of the bridge to turbulent wind may be determined following the well established statistical spectral method originally proposed by Davenport [5]. The method incorporates features such as background response, resonant response, coherence of the turbulent wind, modal coupling, aerodynamic admittance of the structure and aerodynamic damping generated by the structure. The theory has been developed over the years by Davenport and co-workers as well as by others. The buffeting analysis carried out in IBDAS uses Davenport's method.

Davenport's buffeting theory assumes that the total structural response will be a combination of the response for each structural mode as excited by the turbulent wind.

All bridge elements mentioned in section 2.1, i.e. girder, tower legs, main cables and hanger contributes to the mean wind as well as the buffeting response. In the computations of the buffeting response all the above elements are thus treated according to the quasi-steady approach as proposed by Davenport.

As the Davenport buffeting theory relies on the validity of quasi-steady linearization of the aerodynamics of the various bridge components possible non linear behaviour of the component wind load coefficients are not accounted for in the frequency domain analysis.

## 3.2 Time-domain (buffeting simulations)

The shortcoming of linearity of the aerodynamic loads with wind inherent in the frequency domain analyses can be lifted if the dynamic response of the bridge is calculated in the time domain. To this end, time histories of the fluctuating wind must be known in a number of representative locations on the bridge. More over, the wind time series must represent the intensity and the spatial correlation of the turbulence at the bridge site.

A total number of 369 nodes have been selected on the bridge structure as shown in Figure 3.1, for which instantaneous wind speed time series for all 3 global directions have been established using Monte Carlo simulation of the wind field. The time series was received from SdM.

The mean wind direction is horizontal and perpendicular to the bridge axis (y-dir).

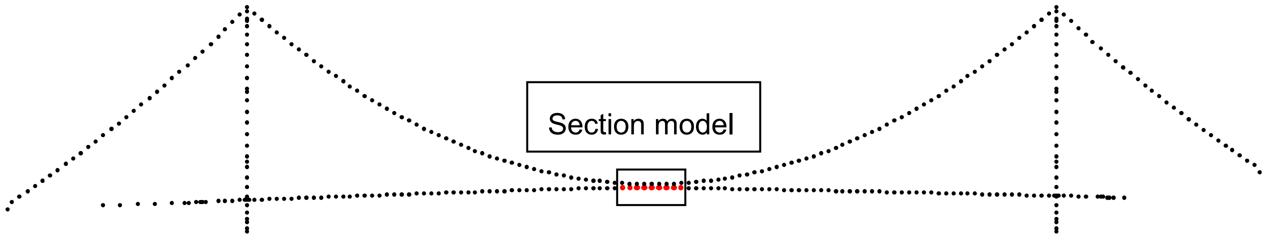


*Figure 3.1 Overview of the nodes selected on the bridge for time series input.*

The analysis requires that the wind speed is defined for all elements on the structure at all time steps. The wind speeds are defined in the 369 nodal points and then extrapolated to give the information on wind speeds for all elements on the whole bridge structure. The 9 central nodes for the deck are used to evaluate the time history response for the section model, the nodes are marked in Figure 3.1.

The number of samples in the time series varies between the limit states as shown below.

| | SLS1 | SLS2 | ULS | SILS |
|---|---|---|---|---|
| Time steps | 2208 | 2017 | 1986 | 2209 |

With sample rate of 10 Hz the average time series length is 3.5 minunte.

The analysis considers the varying angle of attack of the wind onto the girder section, see figure below. This means that the drag, lift and moment coefficients are evaluated at each time step for varying angles of attack between wind and girder including the effect of a change in deck rotation at each time step as outlined in section 2.2.2.

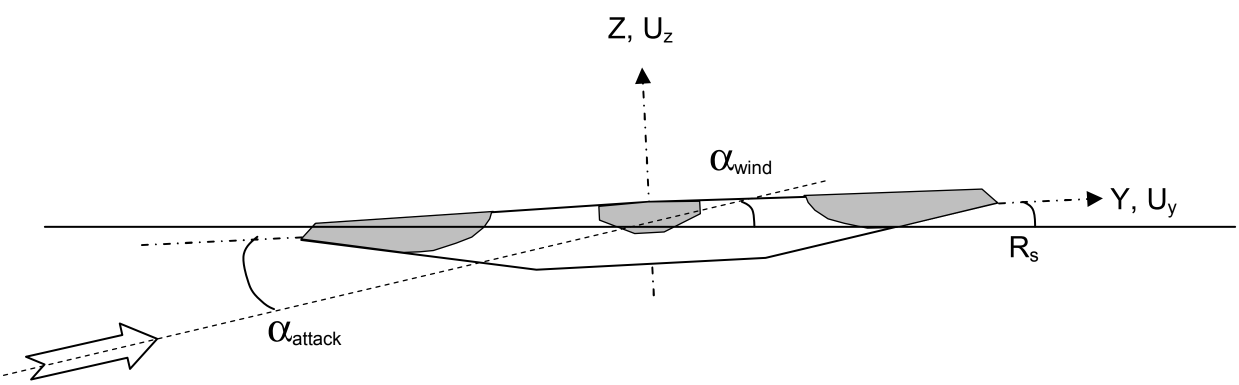


*Figure 3.2 Definition of angle of attack of the wind assumed in the time history analyses.*

The time history analysis does not take admittance, aerodynamic damping derived from aerodynamic derivatives or wind induced reductions in stiffness into account.

# 4 Validation of buffeting analyses vs. section model tests

The deck section model tests carried out at FORCE [6] and BLWTL [4] are used to establish the validity of the frequency domain and time domain buffeting analyses described above.

## 4.1 Computation of dynamic response of the FORCE section model

### 4.1.1 Frequency and time domain responses

The turbulence intensities, spectra and coherences applied in the calculations below are identical to the turbulence properties measured in the FORCE section model test. Figure 4.1 and Figure 4.2 show a comparison of the frequency response (vertical and torsion displacement) of the basic vertical and torsion mode as function of wind speed compared to experimental results.

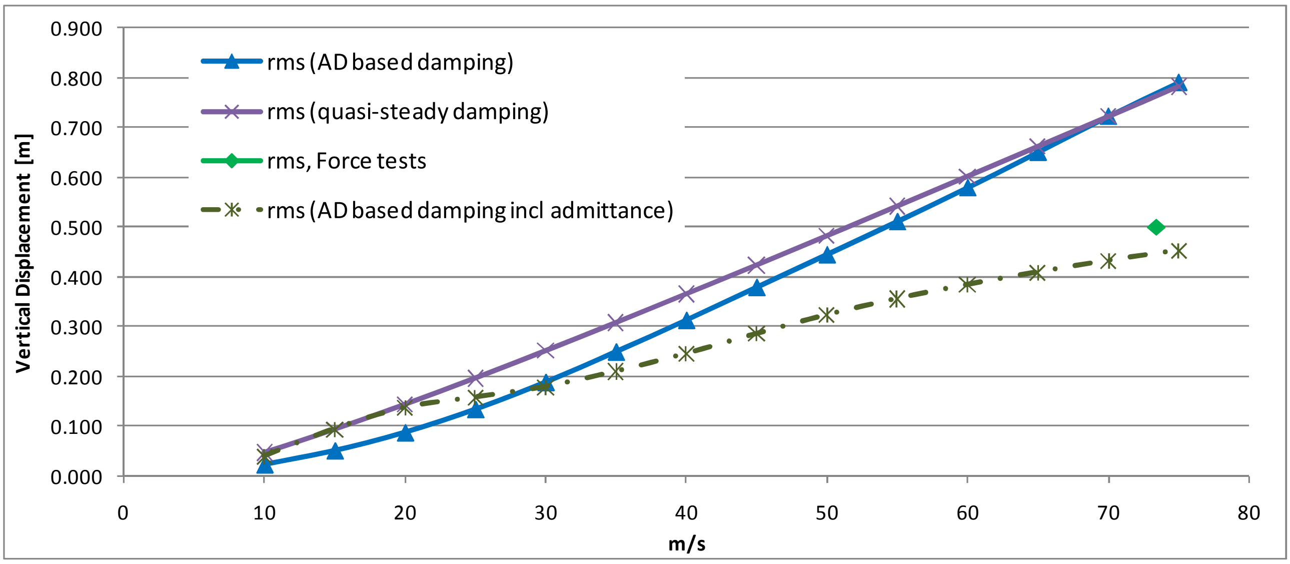


*Figure 4.1 Vertical response $U_z$ obtained from frequency domain buffeting calculations and wind tunnel tests at FORCE.*

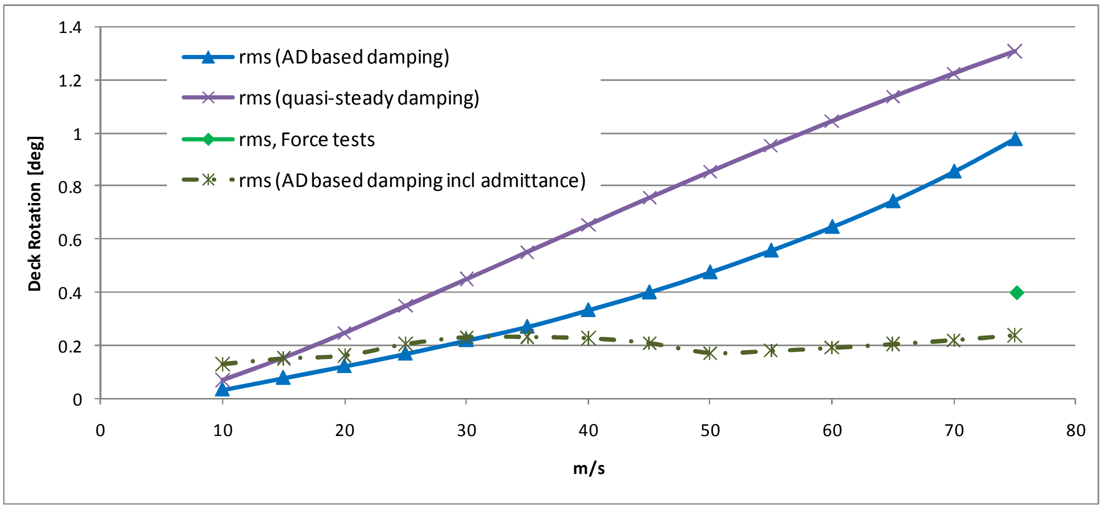


*Figure 4.2 Torsion response $R_s$ obtained from frequency domain buffeting calculations and wind tunnel tests at FORCE .*

From Figure 4.1 and Figure 4.2 it is noted that the vertical and torsion rms responses exceed the measured responses in the wind tunnel. In particular it is noted that the torsion response using quasi-steady aerodynamic damping is almost twice that of the torsion response obtained applying the measured aerodynamic derivatives for determination of the torsion damping. In case of the vertical response a good agreement is noted between the quasi-steady approach and the aerodynamic derivatives. The difference in torsion response is shown in Figure 4.2 is supported by calculating the ratio of aerodynamic damping obtained from the quasi-steady approach $\zeta_{a\theta}^{qs}$ and aerodynamic derivatives $\zeta_{a\theta}^{AD}$:

$$\frac{\zeta_{a\theta}^{qs}}{\zeta_{a\theta}^{AD}} = \frac{\frac{\partial C_M}{\partial \alpha} \cdot U}{16\pi \cdot f_\theta \cdot (-A_2^*) \cdot B}$$

Inserting the appropriate constants for the ULS condition in the above expression yields $\zeta_{a\theta}^{qs}$ / $\zeta_{a\theta}^{AD}$ = 0.172. Knowing that buffeting response is inversely proportional to the square root damping suggests that the quasi-stationary buffeting response shall be at the order of 2.4 times higher than the buffeting response obtained when including the aerodynamic derivatives.

The overshoot of the computed buffeting response applying the aerodynamic derivatives in comparison with the measured responses is attributed in part to the omission of the aerodynamic admittances.

A comparison between responses obtained from the time domain analysis and the frequency domain analyses for the SILS condition (mean wind speed of 60 m/s at 70 m level) is shown in Figure 4.3 and Figure 4.4. From the comparison it is noted that the frequency domain analysis predicts larger responses than the time domain approach. It is also noted that applying aerodynamic torsion damping based on the quasi-steady approach yields larger frequency domain responses than obtained from the aerodynamic derivatives as was also reflected in Figure 4.2.

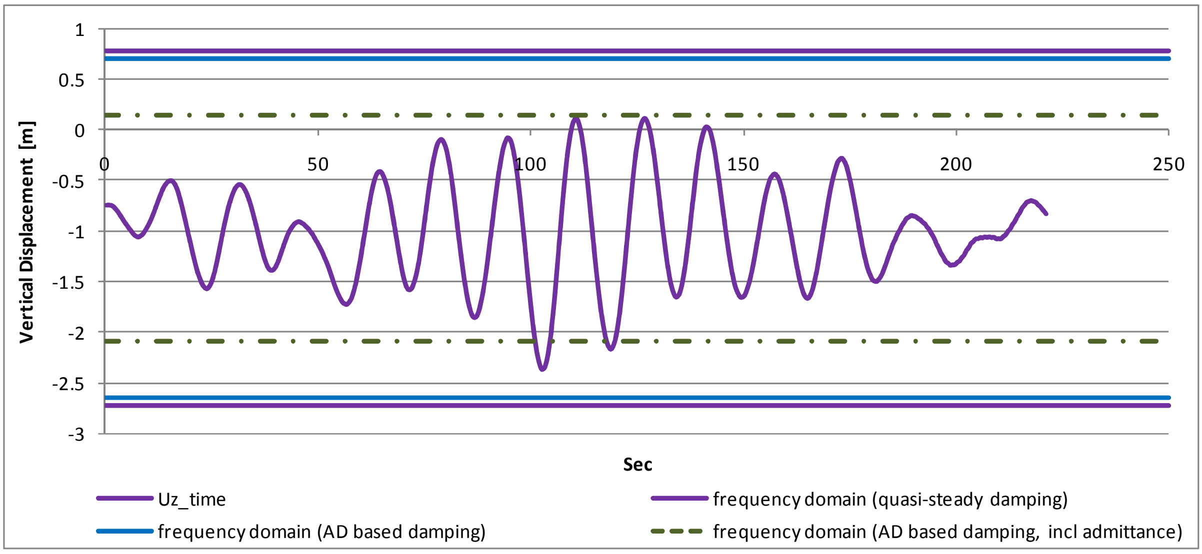


*Figure 4.3 Comparison of vertical response $U_z$ obtained from frequency domain and time domain buffeting analyses.*

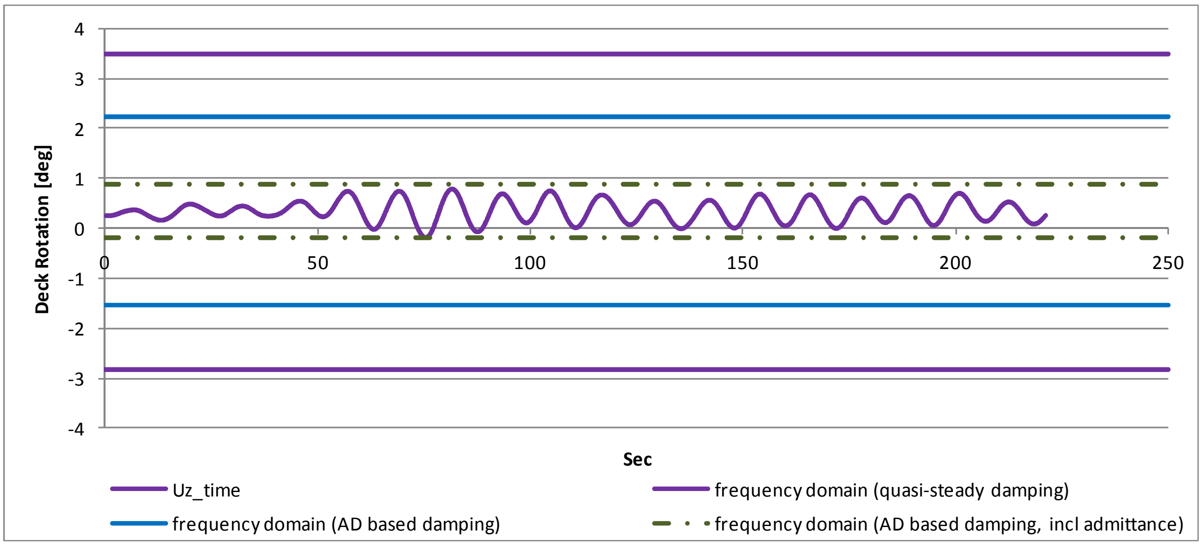


*Figure 4.4 Comparison of torsion response $R_s$ obtained from frequency domain and time domain buffeting analyses.*

It is well known that increasing wind loading on a bridge structure will cause loss of structural stiffness and thus lead to decreasing structural eigenfrequencies. This effect is accounted for in the frequency domain buffeting analysis including aerodynamic damping from the measured aerodynamic derivatives, but is not taken into account in the time domain buffeting computations. In conventional frequency domain buffeting analysis each structural mode is treated separately as a one-degree-of-freedom oscillator, thus modes will not interact as is the case for classical flutter where the torsion frequency will decrease until at resonance with the frequency of the corresponding vertical mode. The interaction between torsion and vertical modes is facilitated by the so-called cross term aerodynamic derivatives $A_1^*$ and $H_3^*$ in the flutter equations. From experience the cross terms are not important for wind speeds much below the flutter speed and as such they are not deemed to be important for buffeting calculations. To substantiate this, Table 4.1 below lists the frequency ratio obtained going from no wind conditions (0 m/s) to SILS (60 m/s) for the fundamental vertical and torsion frequency obtained.

*Table 4.1 Frequency reduction going form zero wind conditions to SILS*

| Mode | Buffeting routine SILS, damping based on AD's | AMC flutter routine SILS |
|---|---|---|
| Vertical | $f_{60} / f_0 = 0.97$ | - |
| Torsion | $f_{60} / f_0 = 0.85$ | - |
| Average | $f_{60} / f_0 = 0.91$ | $f_{60} / f_0 = 0.90$ |

From Table 4.1 it is noted that the frequency reductions are relatively small for wind speeds 30% lower than the flutter speed. Also it is noted that the predicted average loss of stiffness at SILS is almost equal for the buffeting routine and the AMC flutter routine indicating that omission of the cross terms in the frequency domain buffeting analysis has no appreciable effect on the response results. Should it prove interesting to assess the possible effect of the cross terms on the aerodynamic damping, it is possible to estimate the apparent average damping from a flutter prediction and then adjust the vertical and torsion aerodynamic damping accordingly.

#### 4.1.2 Turbulence field, FORCE

The turbulence conditions, i.e. intensities, spectral distributions and cross wind coherences are obviously very important for the resulting buffeting response of the deck cross section. In order to appreciate the comparison of frequency domain and time domain buffeting analyses for the section model it is of interest to review the turbulence properties in the section model tests which are applied for the frequency domain calculations for the section model and the turbulence properties of the time domain analysis which are simulated according to the spectral properties specified by SdM in the basis of design [7]. Figure 4.5 compares the power spectral distributions normalized by mean wind speed squared as applied in the frequency and time domain analyses. Table 4.2 compares the relevant length scales and coherence decay exponents.

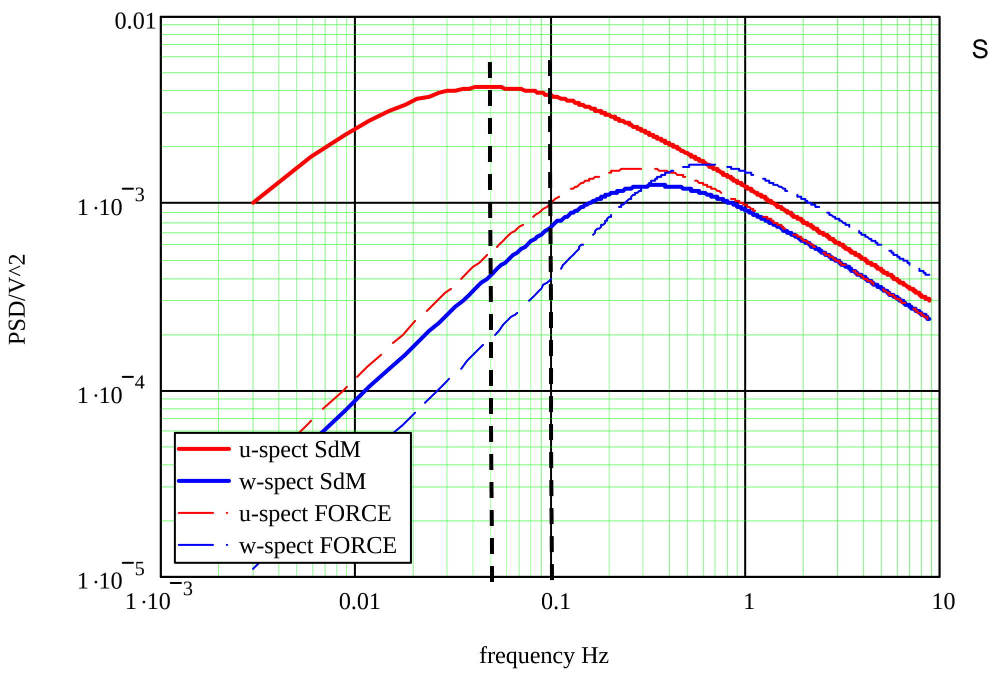


*Figure 4.5 Power spectral distributions of longitudinal and vertical turbulence normalized by mean wind speed squared. SdM specification (thick solid lines), FORCE (thin dashed lines).*

*Table 4.2 Turbulence properties FORCE and SdM.*

| | Length scale | | Intensity | | Exponent | |
|---|---|---|---|---|---|---|
| Direction | FORCE | SdM | FORCE | SdM | FORCE | SdM |
| Along wind u | $L_u$ = 30 m | $L_u$ = 177 m | $I_u$ = 7.4% | $I_u$ = 13.8% | $C_{uy}$ = 7.5 | $C_{uy}$ = 10 |
| Vertical w | $L_w$ = 10 m | $L_w$ = 44 m | $I_w$ = 7.5% | $I_u$ = 6.9% | $C_{wy}$ = 5 | $C_{wy}$ = 6.5 |

For the vertical turbulence (w) spectrum which drives the vertical and torsion motions, it is noted that the specifications by SdM overshoots the FORCE spectrum by approximately a factor of 2 in the frequency range 0.05 - 0.1 Hz which is of interest for the deck section vertical and torsion response. Thus it is expected that the time domain analysis should overestimate the frequency domain response by a factor of 1.4, which is partially balanced by the fact that the along span coherence exponent of vertical turbulence estimated for the FORCE turbulence $C_{wy}$ = 5 is larger than the SdM specification $C_{wy}$ = 6.5. In summary it is concluded that the vertical turbulent wind loading obtained from the SdM specifications and FORCE measurements in the important 0.05 - 0.1 Hz frequency range are in fairly good agreement.

## 4.2 Computation of dynamic response of the BLWTL section model

### 4.2.1 Frequency and time domain responses

The BLWTL section model was spring suspended in all three degrees of freedom (y, z and Rs) thus analysis of the response of this model provided a means for comparison of measured and calculated horizontal responses. Figure 4.6, Figure 4.7 and Figure 4.8 show a comparison of the frequency response (vertical, transversal and torsion displacement) of the basic vertical and torsion mode as function of wind speed compared to experimental results

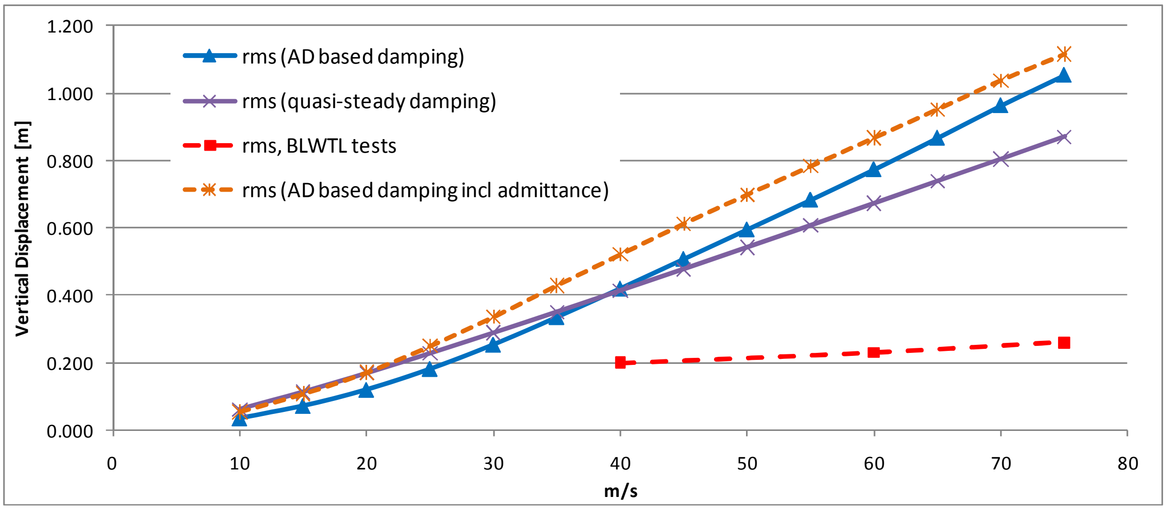


*Figure 4.6 Vertical response $U_z$ obtained from frequency domain buffeting calculations and wind tunnel tests at BLWTL.*

From Figure 4.6 it is noted that the predicted vertical response obtained using either quasi-steady or aerodynamic derivatives based aerodynamic damping is quite similar and approximately three times higher than measured at BLWTL.

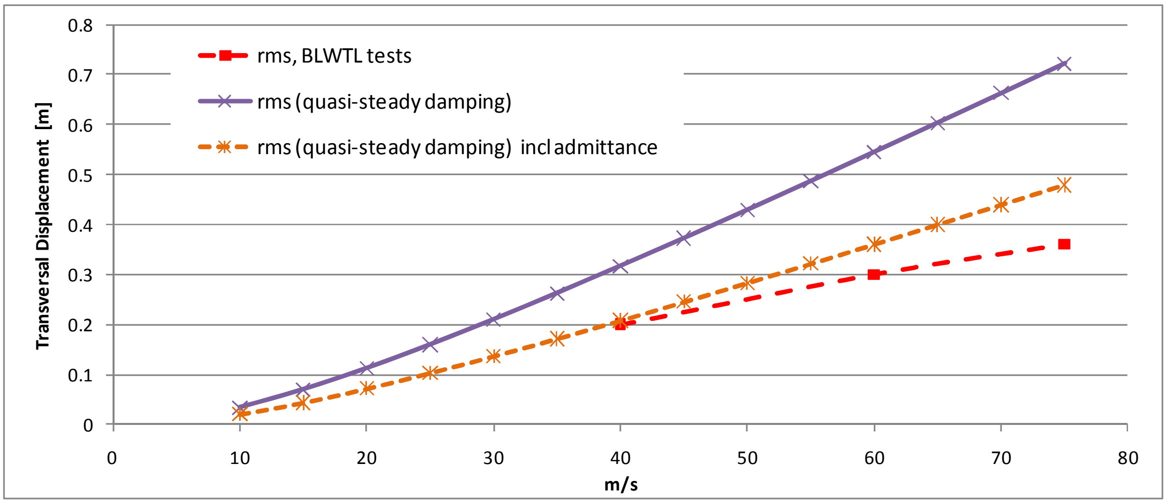


*Figure 4.7 Transversal (along wind horizontal) response $U_y$ obtained from frequency domain buffeting calculations and wind tunnel tests at BLWTL.*

The calculated quasi-steady transversal (along wind) response, Figure 4.7, overshoots the measurements but becomes in good agreement if the aerodynamic admittance is introduced.

The frequency domain torsion response, Figure 4.8, is much larger when calculated based on the quasi-steady damping than calculated using the aerodynamic derivatives for determining the torsion damping which is similar to what was found for the FORCE buffeting response measurements. Adding the aerodynamic admittance increases the calculated response slightly.

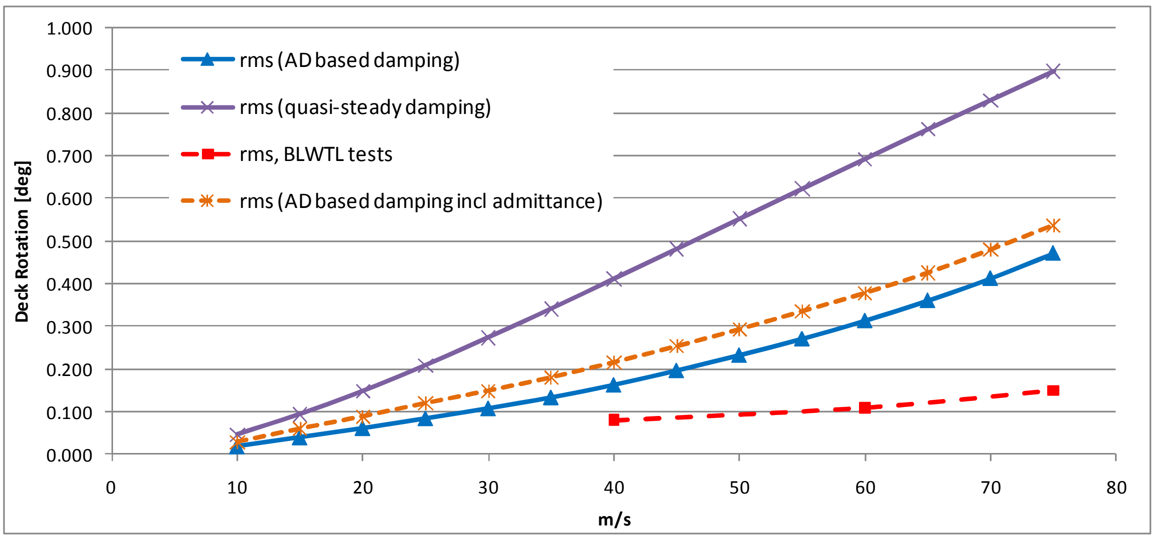

*Figure 4.8 Torsion response $R_s$ obtained from frequency domain buffeting calculations and wind tunnel tests at BLWTL.*

Time domain analyses of the section model giving vertical, transversal and torsion displacement responses based on the SdM turbulence specifications are shown in Figure 4.9, Figure 4.10 and Figure 4.11. From these plots it is noted that the vertical and torsion response is well within the bounds given by the quasi-steady frequency domain analysis.

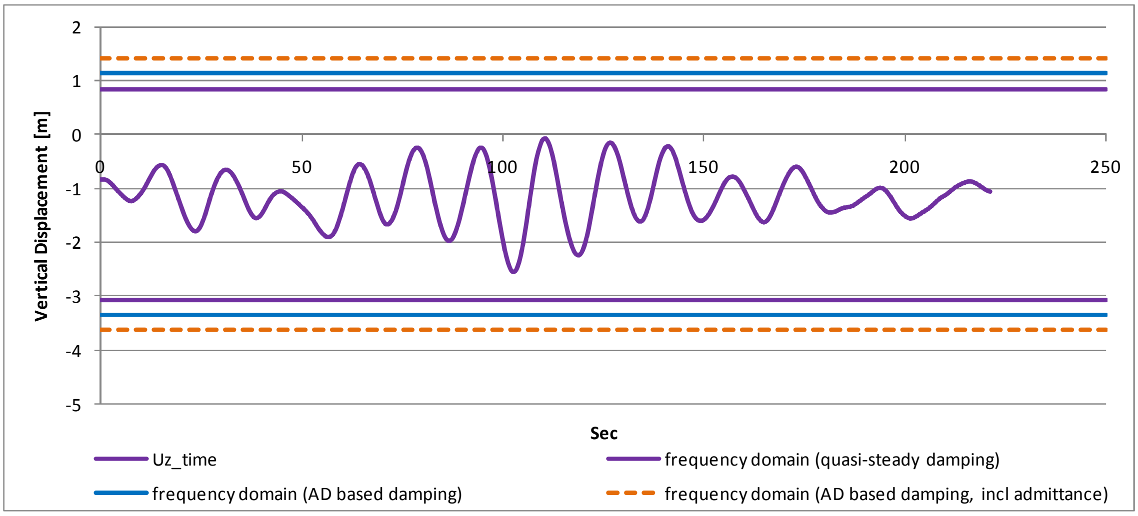


*Figure 4.9 Comparison of vertical response $U_z$ obtained from frequency domain and time domain buffeting analyses.*

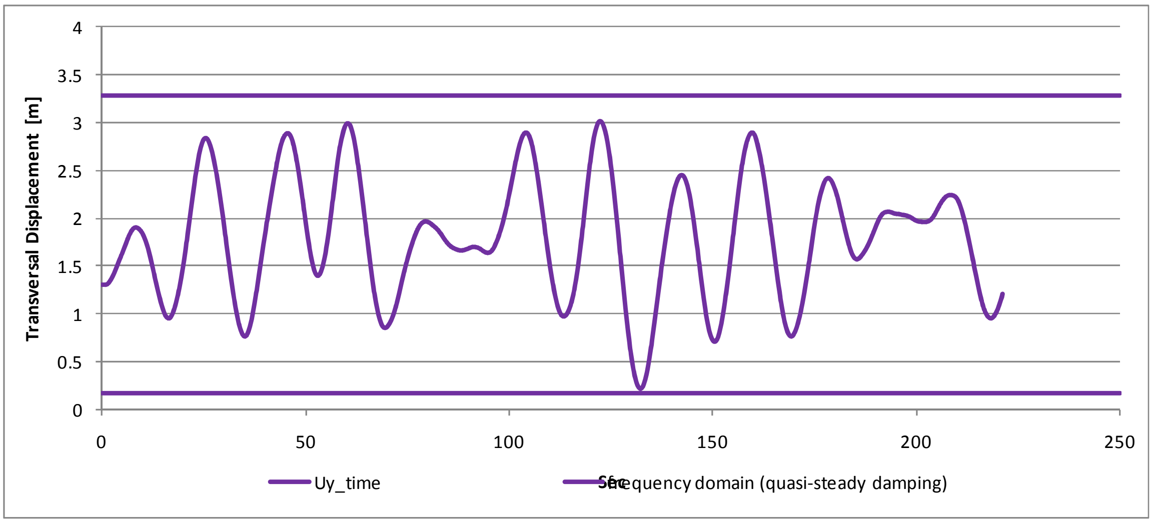


*Figure 4.10 Comparison of transverse (along wind) response $U_y$ obtained from frequency domain and time domain buffeting analyses.*

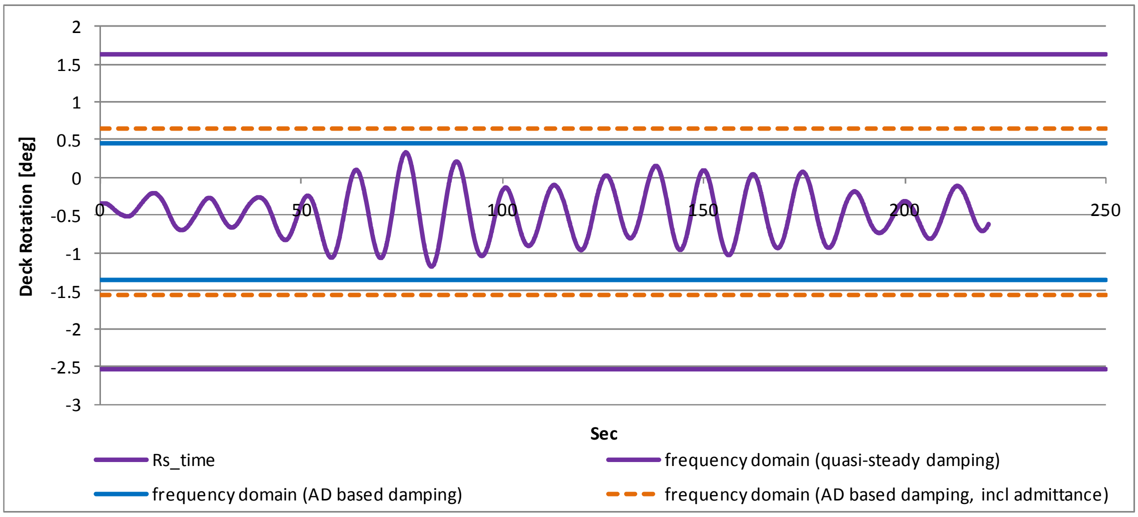


*Figure 4.11 Comparison of torsion response $R_s$ obtained from frequency domain and time domain buffeting analyses.*

### 4.2.2 Turbulence field, BLWTL

Figure 4.12 compares the BLWTL power spectral distributions normalized by mean wind speed squared as applied in the frequency and time domain analyses. Table 4.3 compares the relevant length scales and coherence decay exponents.

*Table 4.3 Turbulence properties BLWTL and SdM.*

| | Length scale | | Intensity | | Exponent | |
|---|---|---|---|---|---|---|
| Direction | BLWTL | SdM | BLWTL | SdM | BLWTL | SdM |
| Along wind u | $L_u$ = 11 m | $L_u$ = 177 m | $I_u$ = 11.7% | $I_u$ = 13.8% | $C_{uy}$ = 7.4 | $C_{uy}$ = 10 |
| Vertical w | $L_w$ = 5 m | $L_u$ = 44 m | $I_w$ = 10% | $I_u$ = 6.9% | $C_{wy}$ = 4.8 | $C_{wy}$ = 6.5 |

For the vertical turbulence (w) spectrum which drives the vertical and torsion motions, it is noted that the specifications by SdM overshoots the BLWTL spectrum by approximately a factor of 2 in the frequency range 0.05 - 0.1 Hz which is of interest for the deck section vertical and torsion response. For the along wind response the overshoot is at the order of 10 times. Thus it is expected that the time domain analysis could overestimate the computed section model frequency domain response by as much as a factor of 3.

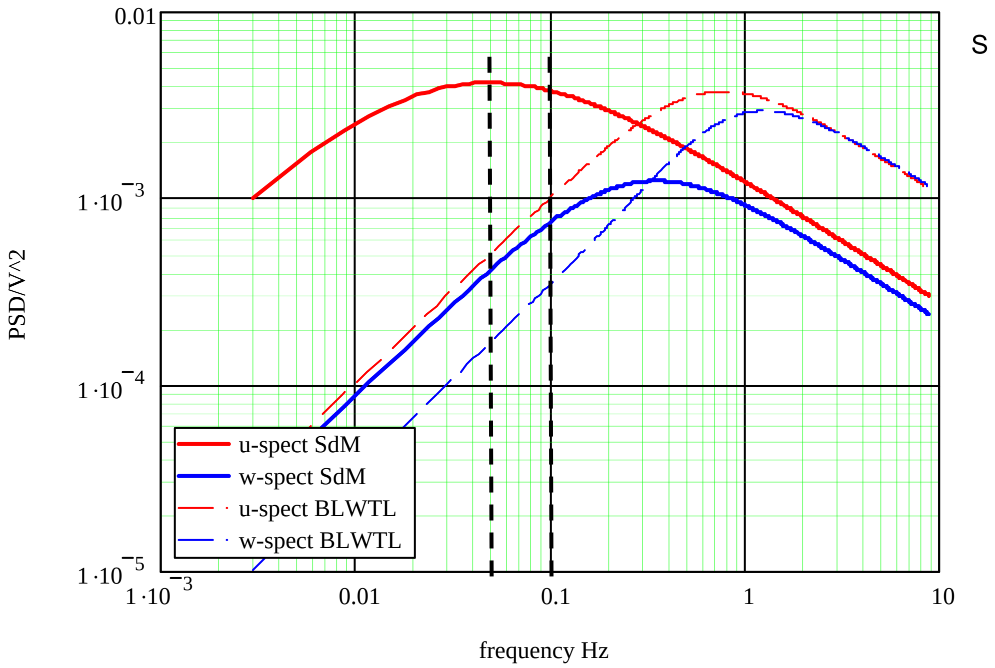


*Figure 4.12 Power spectral distributions of longitudinal and vertical turbulence normalized by mean wind speed squared. SdM specification (thick solid lines), BLWTL (thin dashed lines).*

## 4.3 Conclusions from section model response calculations

From the above section model response calculations the following conclutions are drawn:

- Quasi-steady frequency domain calculations always shows larger responses than frequency domain calculations including measured aerodynamic derivatives and aerodynamic admittances.
- Quasi-steady frequency domain calculations always shows larger responses than measured section model responses.
- Quasi-steady frequency domain calculations always shows larger responses than time domain computations based on quasi-steady aerodynamic damping.

The latter conclusion may in part be due to the fact that only one realisation of the wind time series for each load condition was available and applied and in part to the fact that the received wind time series are shorter than 10 minute time series which are commonly applied for such analyses.

Based on the above conclusions, the following decisions were taken with regards to application of aerodynamic admittances and aerodynamic damping models for the full bridge buffeting calculations.

### 4.3.1 Aerodynamic admittance, AA

An aerodynamic admittance AA(f) = 1 in the entire frequency range will lead to conservative responses calculated for the complete bridge structure and was thus adopted for design load evaluations.

### 4.3.2 Aerodynamic damping, AD

For the vertical and the torsion degrees of freedom aerodynamic damping based on the measured aerodynamic derivatives were found to give the best match with direct measurements. Aerodynamic damping based on the measured aerodynamic derivatives (FORCE) was thus adopted for buffeting frequency domain buffeting calculations for the complete bridge structure used for design load evaluations. The along wind aerodynamic damping was evaluated from quasi-steady assumptions, i.e. the aerodynamic damping is proportional to the drag coefficient at 0 deg. wind incidence.

# 5 Buffeting analyses of the full bridge

This section shows a comparison of the structural response analysed with time domain and Dynwind (frequency domain) for the full bridge.

Only the transverse wind (y+ dir) is considered as the time histories has the primary direction perpendicular to the bridge. The calculated displacements of the structure are in the transverse (y dir), vertical (z dir) and in rotation (Rs dir) degrees of freedom.

## 5.1 Turbulent wind field

The turbulent wind filed in the frequency domain calculations is set up according to the specifications given by SdM [7].

The mean wind frofiles for the SLS1, SLS2, ULS and SLIS conditions are shown in Figuer 5.1.

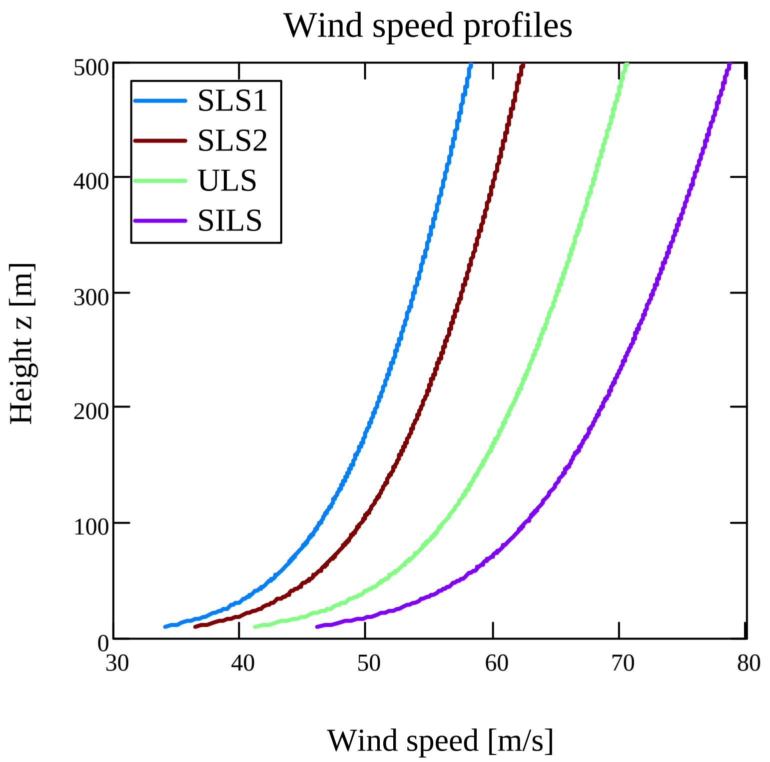


*Figure 5.1 Mean wind speed as function of level above ground*

Turbulent length scale and turbulence intensities are shown in Figure 5.2

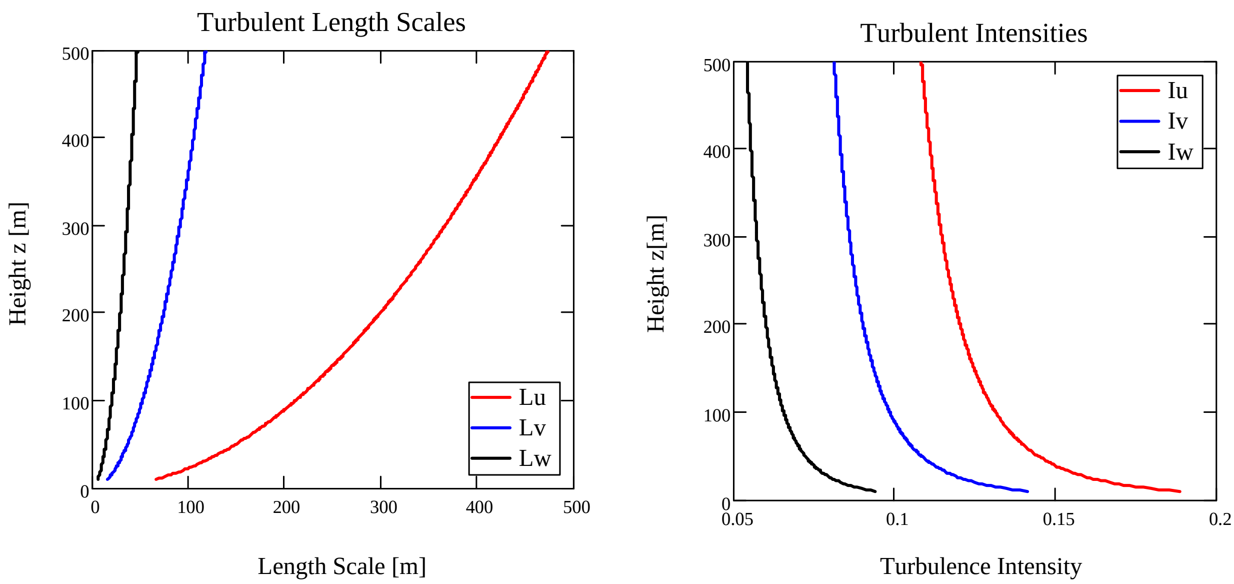


*Figure 5.2 Length scales and turbulence intensities specified by SdM*

Finally the along wind, cross wind and vertical turbulence spectra corresponding to the SILS condition is shown in Figure 5.3

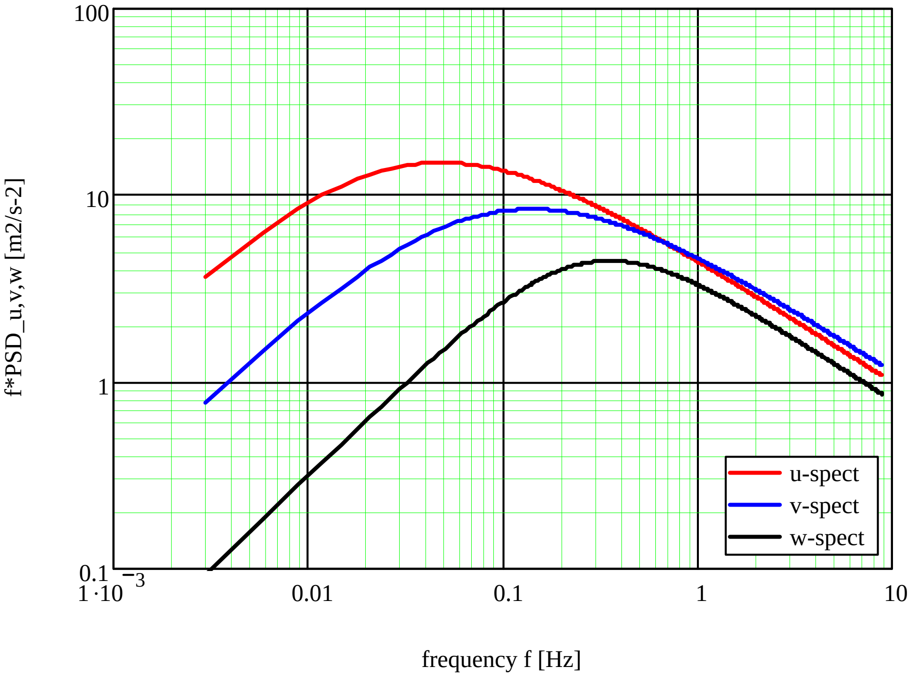


*Figure 5.3 Turbulence spectra for the SILS condition specified by SdM*

The spatial coherence of turbulence is given as conventional exponential expressions with the decay coefficients listed in Table 5.1.

*Table 5.1 Decay exponents specified by SdM*

| Turbulence component | x - along wind dir. | y - cross wind dir. | z - vertical dir. |
|---|---|---|---|
| Along wind u | $C_{ux}$ = 3 | $C_{uy}$ = 10 | $C_{wx}$ = 0.5 |
| Cross wind v | $C_{vx}$ = 3 | $C_{vy}$ = 6.5 | $C_{wy}$ = 6.5 |
| Vertical w | $C_{wx}$ = 0.5 | $C_{wy}$ = 6.5 | $C_{wz}$ = 3 |

## 5.2 Aerodynamic admittances in frequency domain analyses

The frequency domain analysis of the full bridge model have been evaluated using the quasi-steady assumption for the along wind (transversal) aerodynamic damping, but the measured aerodynamic dampings for the vertical and torsion aerodynamic dampings. Three different admittance inputs were used for comparison with the time domain calculations:

1) No Admittance
2) Admittance based on FORCE
3) Admitance based on BLWTL

The time history analysis does not take admittance into account, so these results are directly comparable to the “no admittance” values, save the effect of aerodynamic damping which is likely to be important for the torsion response. Moreover, the “no admittance” frequency domain analysis was applied in the bridge design as this proved to be the most conservative condition.

## 5.3 Mean wind response

The response of structures to turbulent wind calculated in the frequency domain is composed of a static response to the mean wind combined with a dynamic response to the turbulence.

The mean wind response of the bridge girder to the 4 loading conditions investigated is shown in Figure 5.4, Figure 5.5 and Figure 5.6.

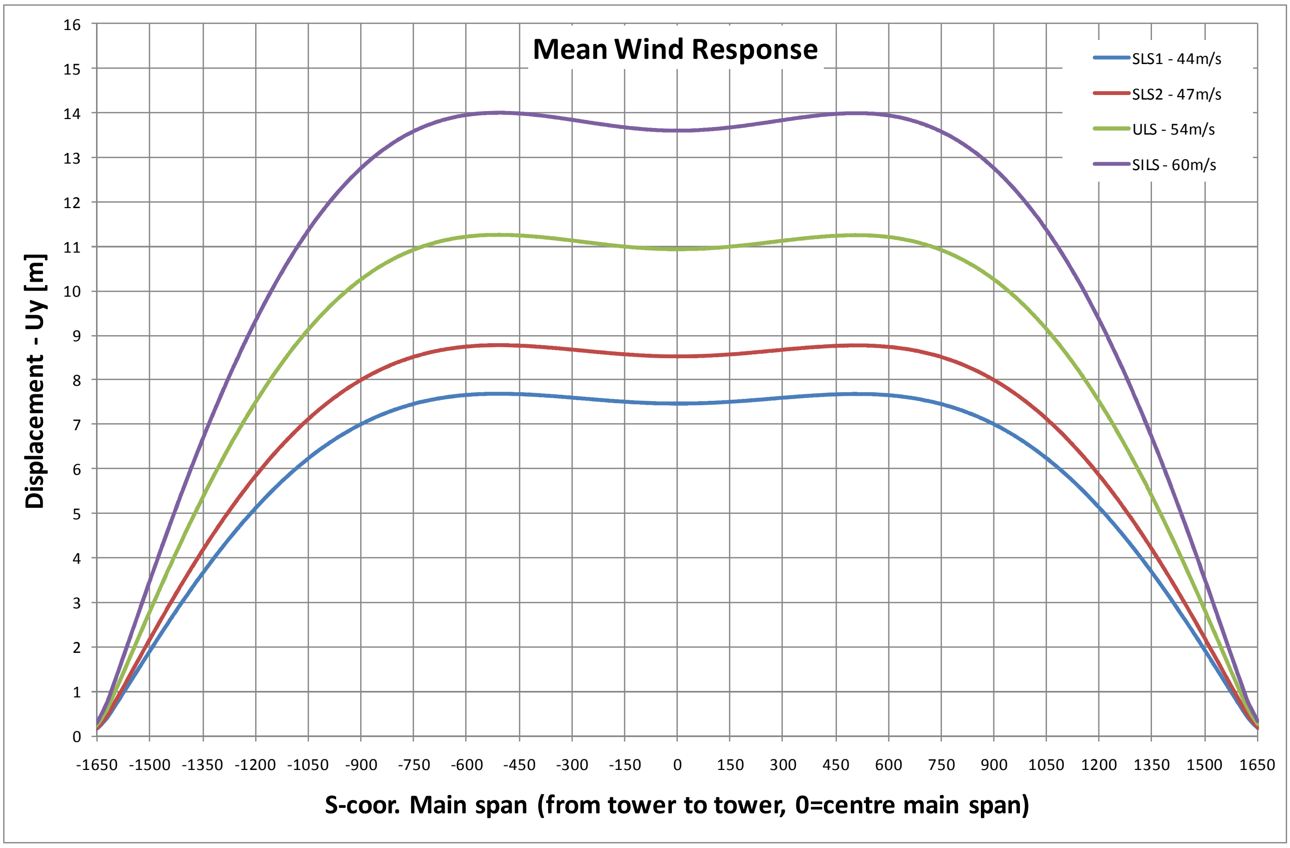


*Figure 5.4 Horizontal (along wind) displacement of the bridge girder for load conditions SLS1, SLS2, ULS and SILS.*

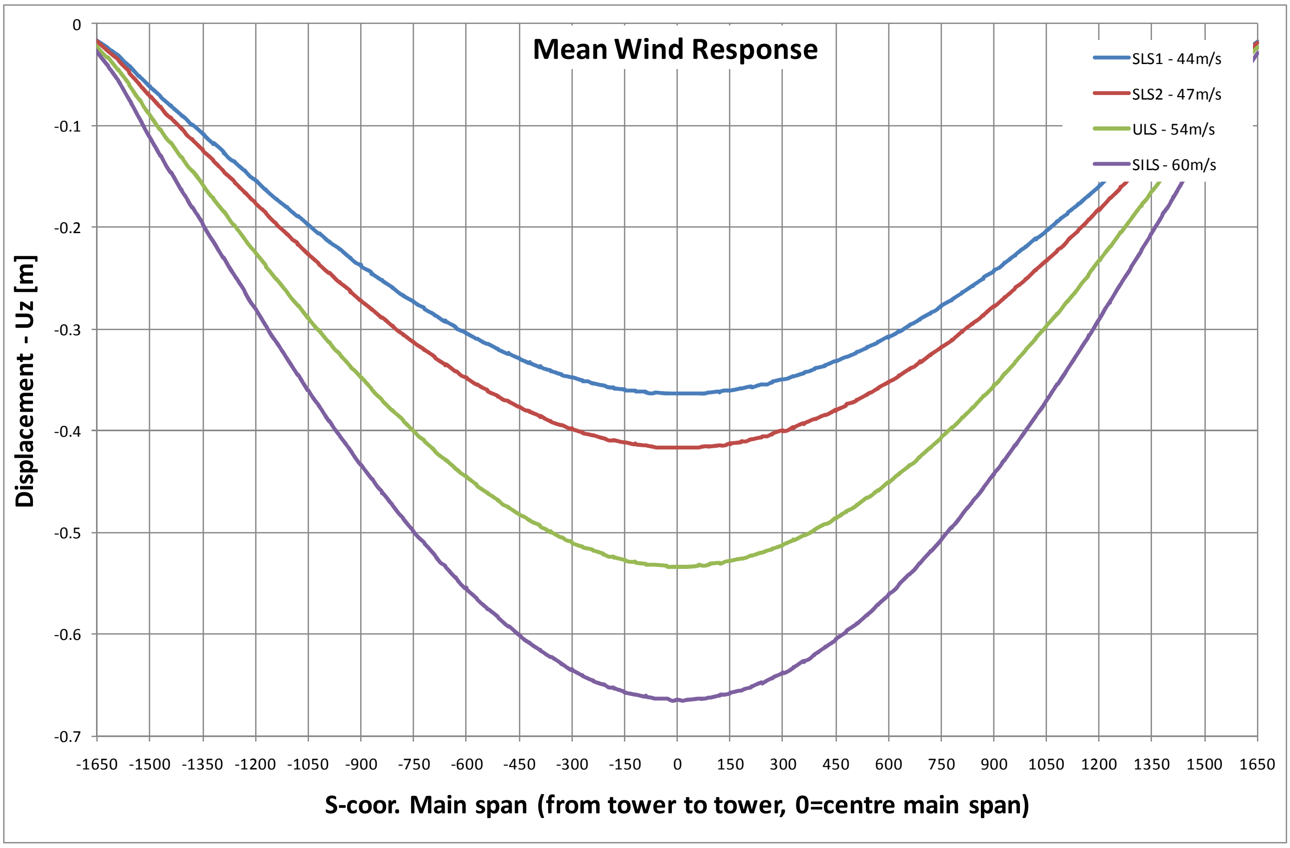


*Figure 5.5 Vertical displacement of the bridge girder for load conditions SLS1, SLS2, ULS and SILS.*

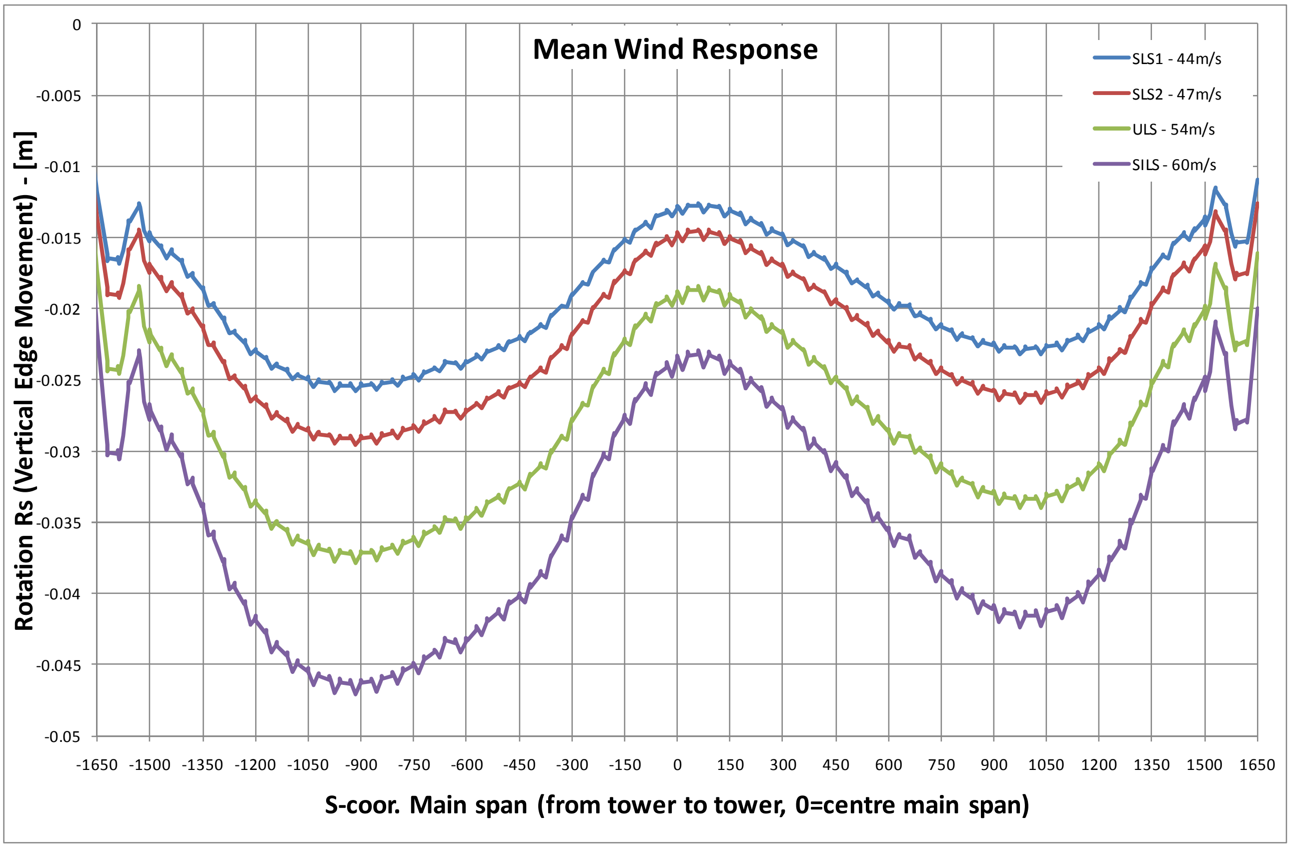


*Figure 5.6 Angular displacement of the bridge girder for load conditions SLS1, SLS2, ULS and SILS.*

## 5.4 Mode shapes in frequency domain analysis

The dynamic response of the bridge is composed mainly of the resonsnant response of a number of different eigen modes of motion excited by the turbulent wind. The dominant frequencies contributing to the dynamic wind response are the first few bending and torsion modes, i.e. below approx 0.2 Hz, as shown in Figure 5.7. The frequency domain computation reported below includes a total of 100 eigen moes.

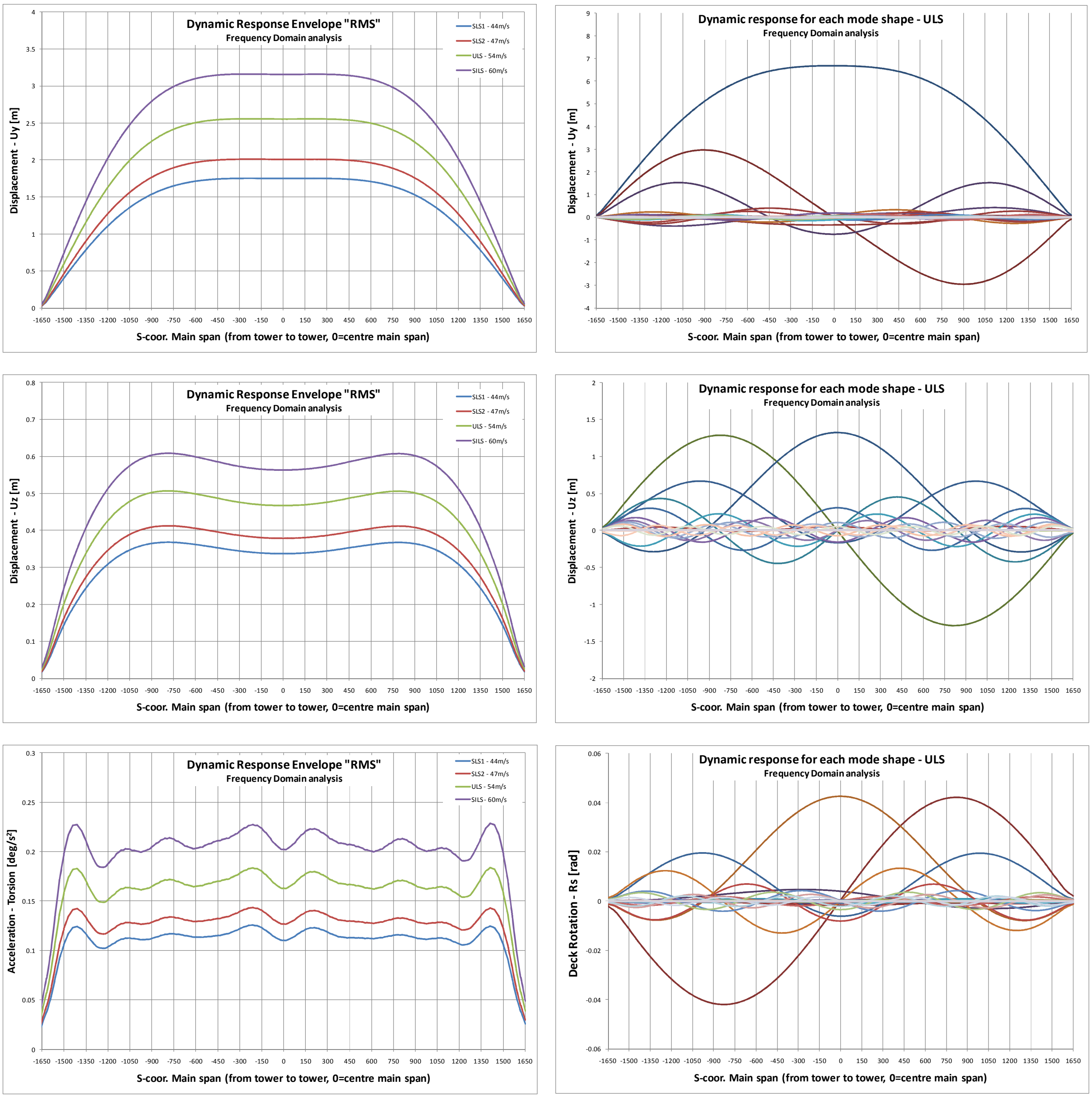


*Figure 5.7 Vertical (lateral), vertical and torsion rms displacements and corresponding dominant modes in the buffeting analysis.*

Although the measured admittances, see section 2.3 and [1], are considerably above 1 for higher frequencies and it may thus seem imperative to use them in the calculations instead of not including admittance at all (i.e. using admittance=1), it is clear from the plots in Figure 5.7 that it is the lower frequencies that dominate the buffeting responses. The frequencies of these lower modes are in the range where the measured admittances are below 1. Therefore, using no admittance will be the conservative choice, as indeed confirmed by the present calculations as it is shown in the following sections.

Calculated Root Mean Square accelerations along the main span are shown in Figure 5.8, Figure 5.9, and Figure 5.10 below.

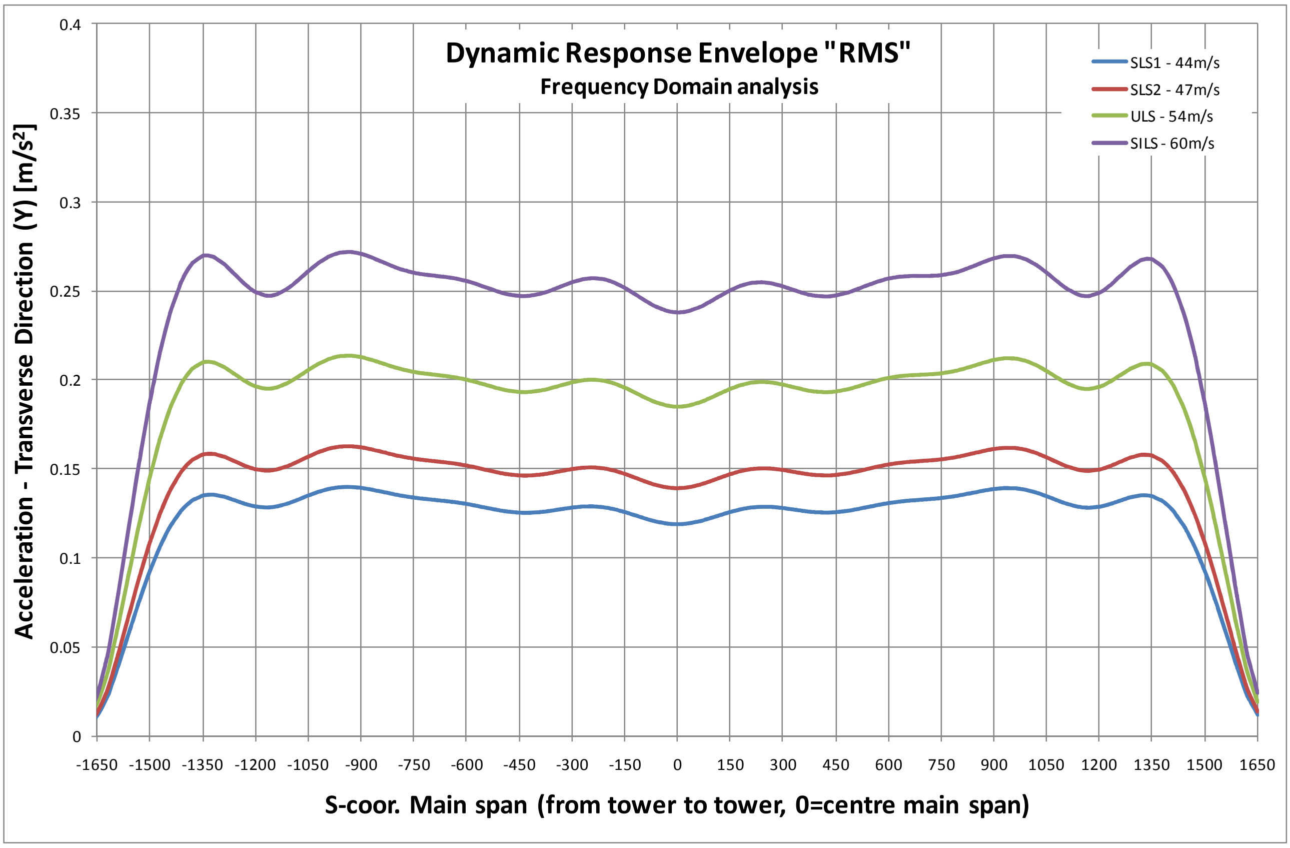


*Figure 5.8 Horizontal RMS accelerations along span.*

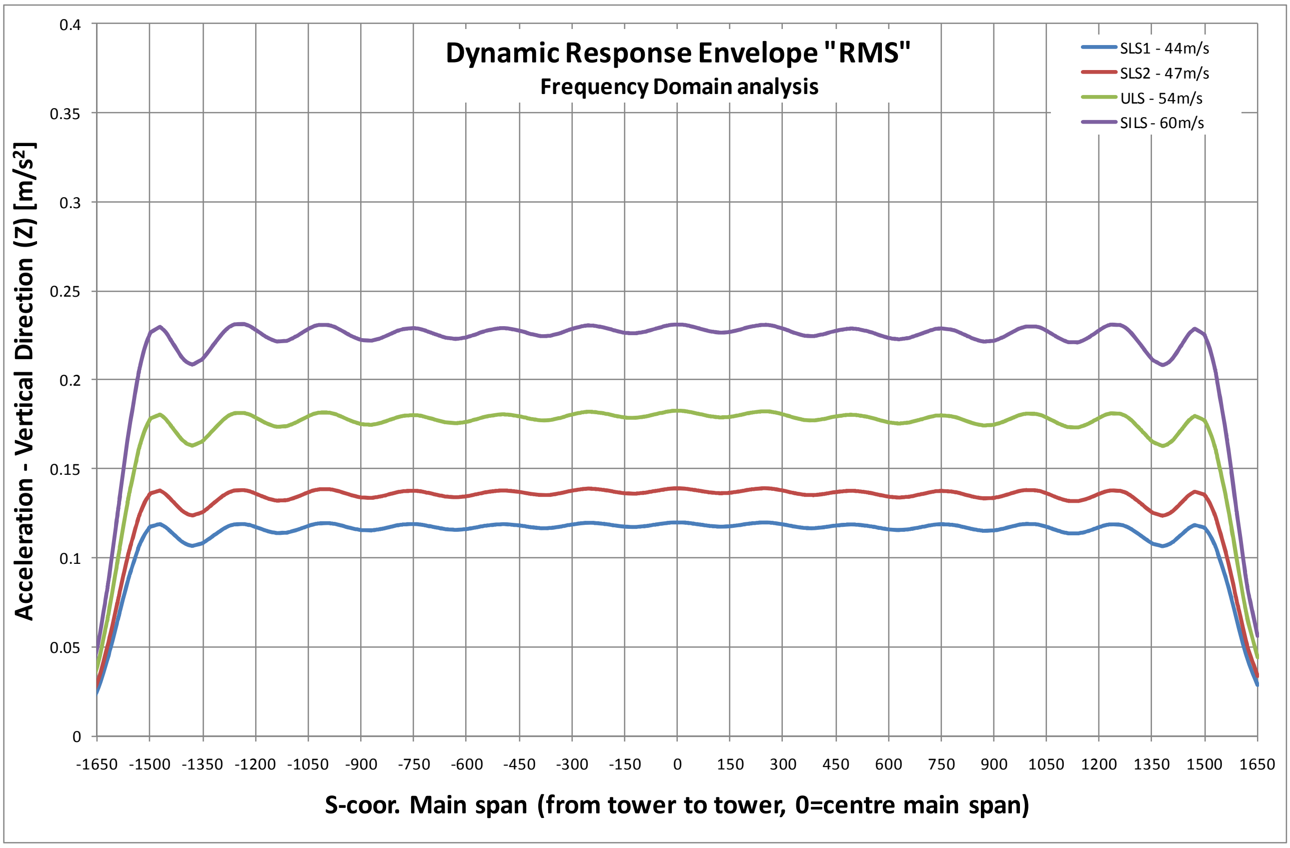


*Figure 5.9 Vertical RMS accelerations along the span at the centre line of the railway girder.*

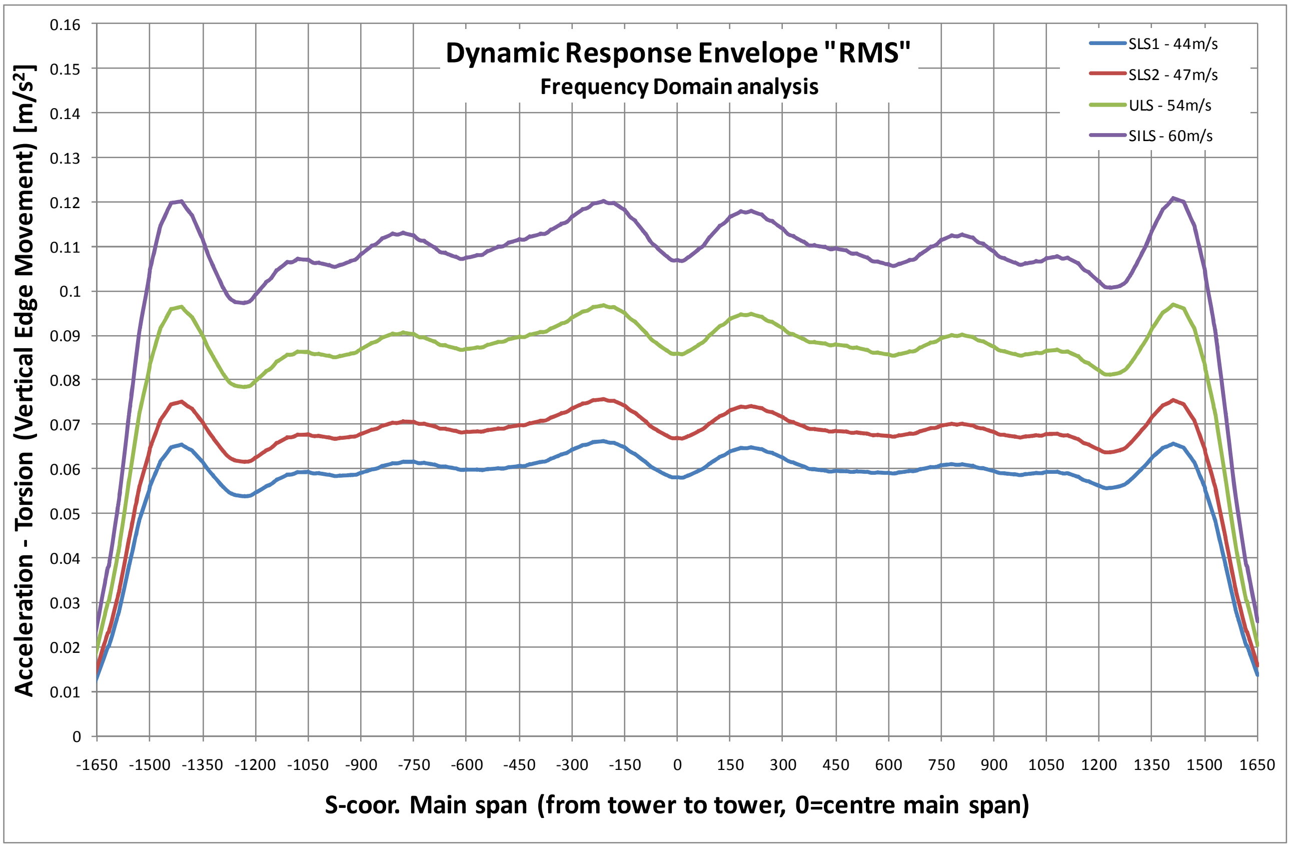


*Figure 5.10 RMS vertical edge deflections along the span due to girder twist.*

## 5.5 Deflections and rotations at centre main span (S = 0)

While the Root Mean Square accelerations are of importance for human comfort, peak displacements are governing for the stresses in the structure.

The result of the buffeting analysis is given in the following figures for load conditions SLS1, SLS2, ULS and SILS. The reported deflections are transverse Uy, vertical Uz and rotation Rs.

It is noted that the subsequent graphs compares frequency domain responses obtained with aerodynamic damping based on the measured aerodynamic derivatives while the time domain responses are based on the quasi-stationary estimates of the aerodynamic damping. With reference to Figure 4.2 it is expected that the time domain simulations overpredict the responses in comparison to the frequency domain computations as the aerodynamic damping in torsion based on the measured aerodynamic derivatives is approximately twice that of the aerodynamic torsion damping based on the quasi-stationary assumption.

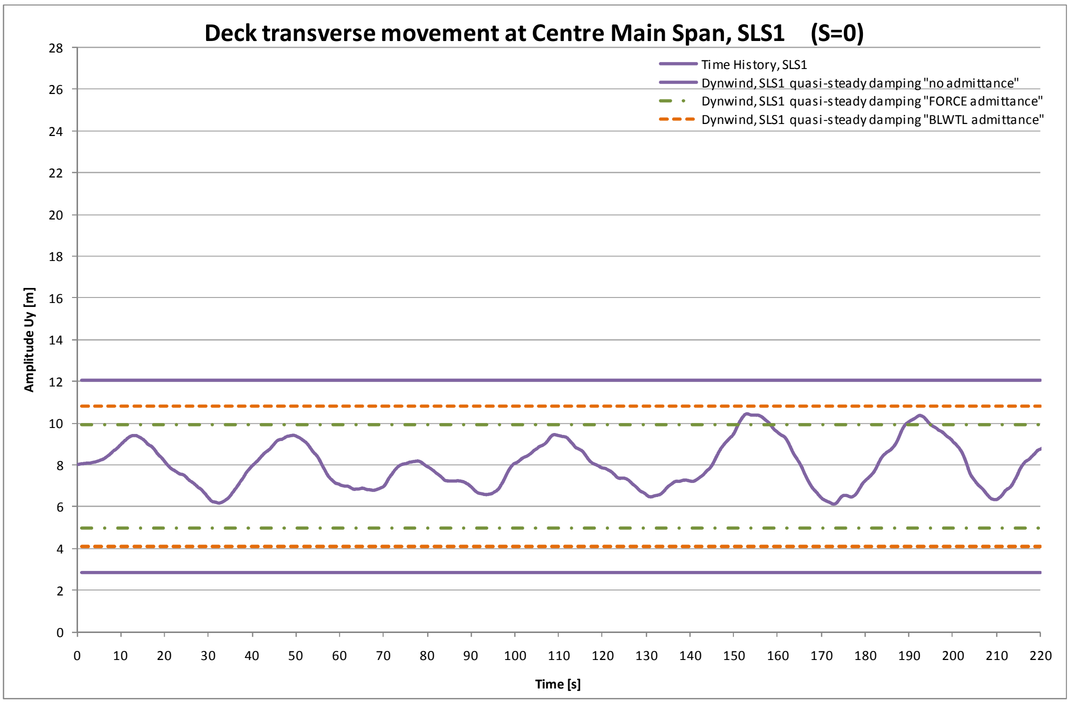


*Figure 5.11 Buffeting comparisons horiztal response, SLS1.*

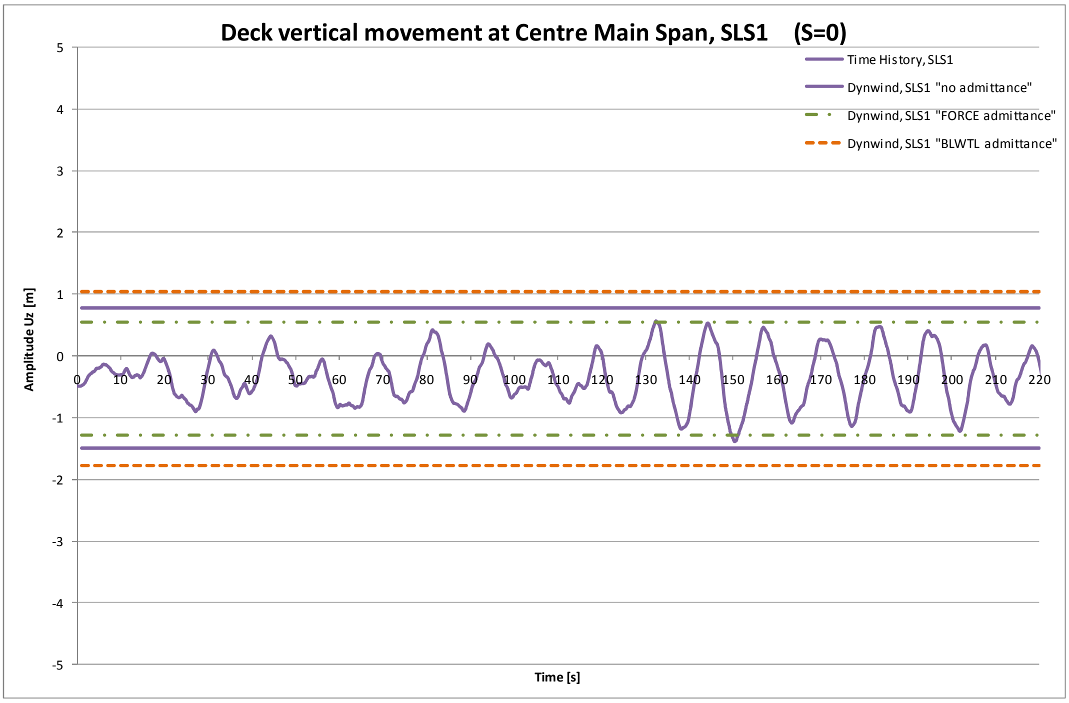


*Figure 5.12 Buffeting comparisons vertical response, SLS1.*

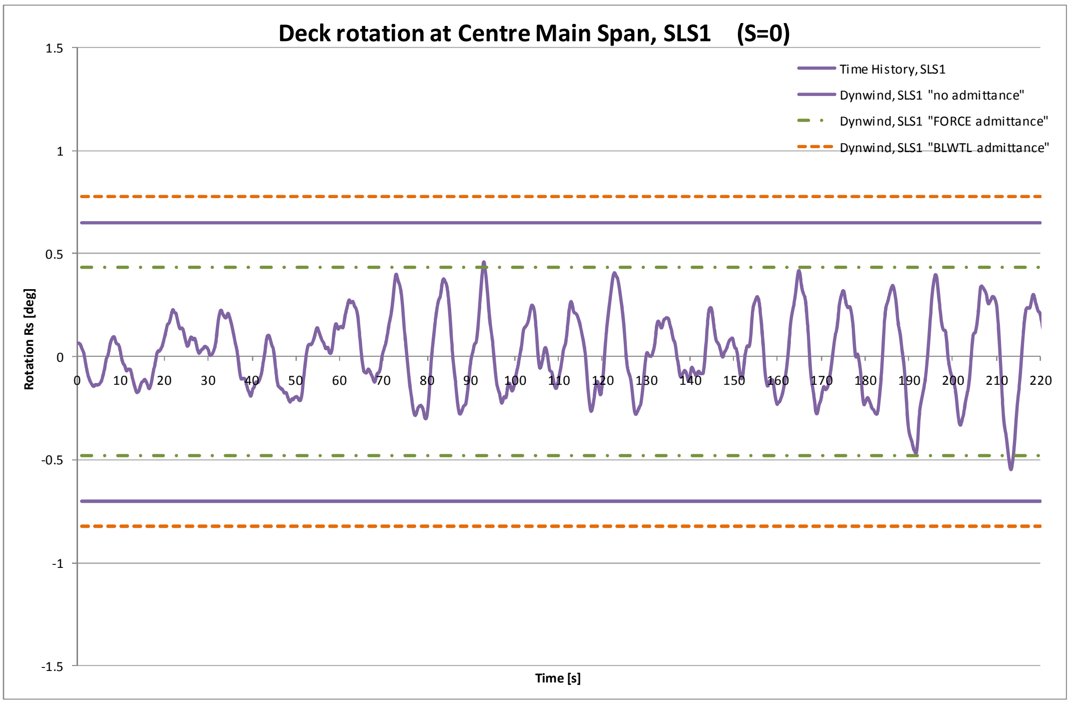


*Figure 5.13 Buffeting comparisons torsion response, SLS1.*

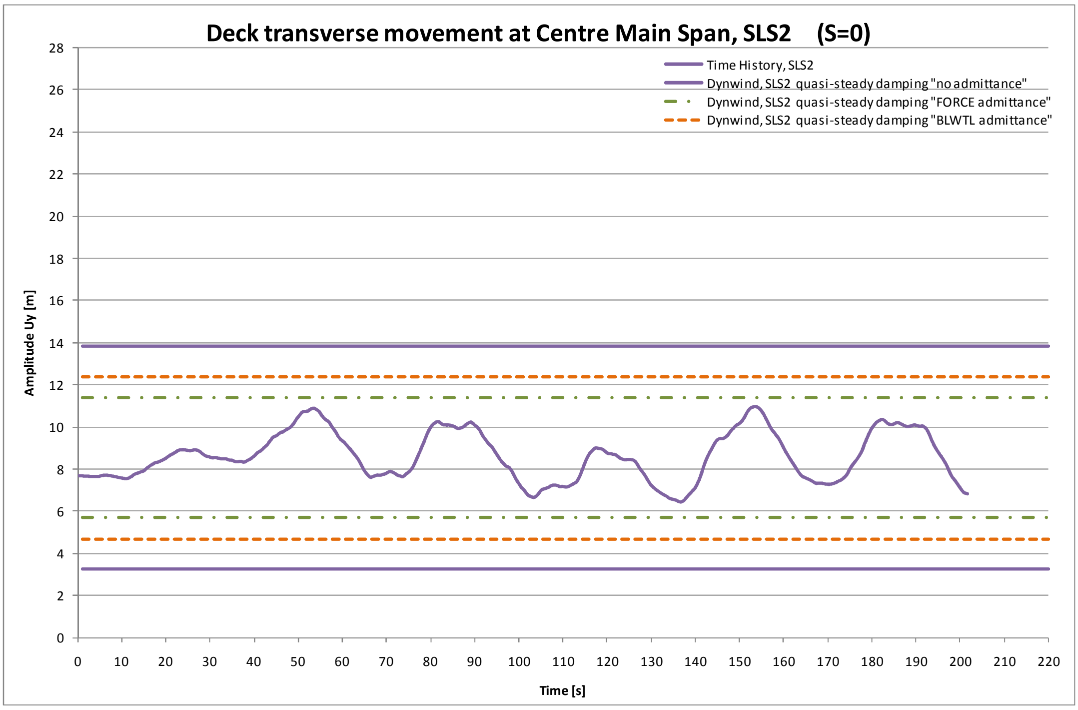


*Figure 5.14 Buffeting comparisons horizontal response, SLS2.*

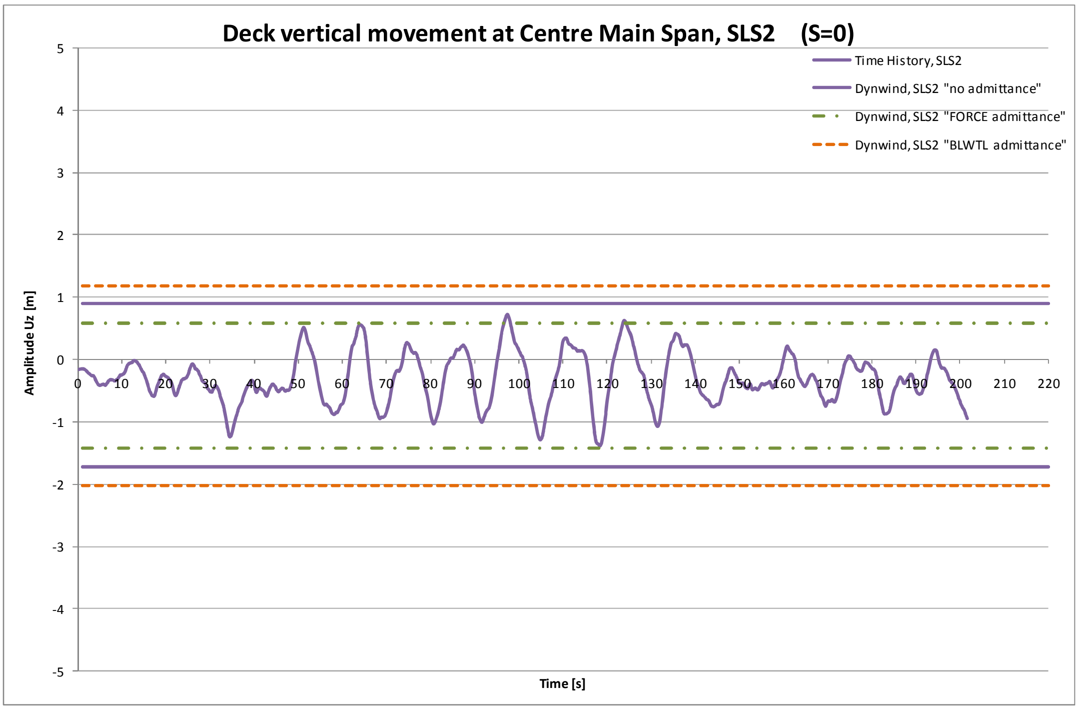


*Figure 5.15 Buffeting comparisons vertical response, SLS2.*

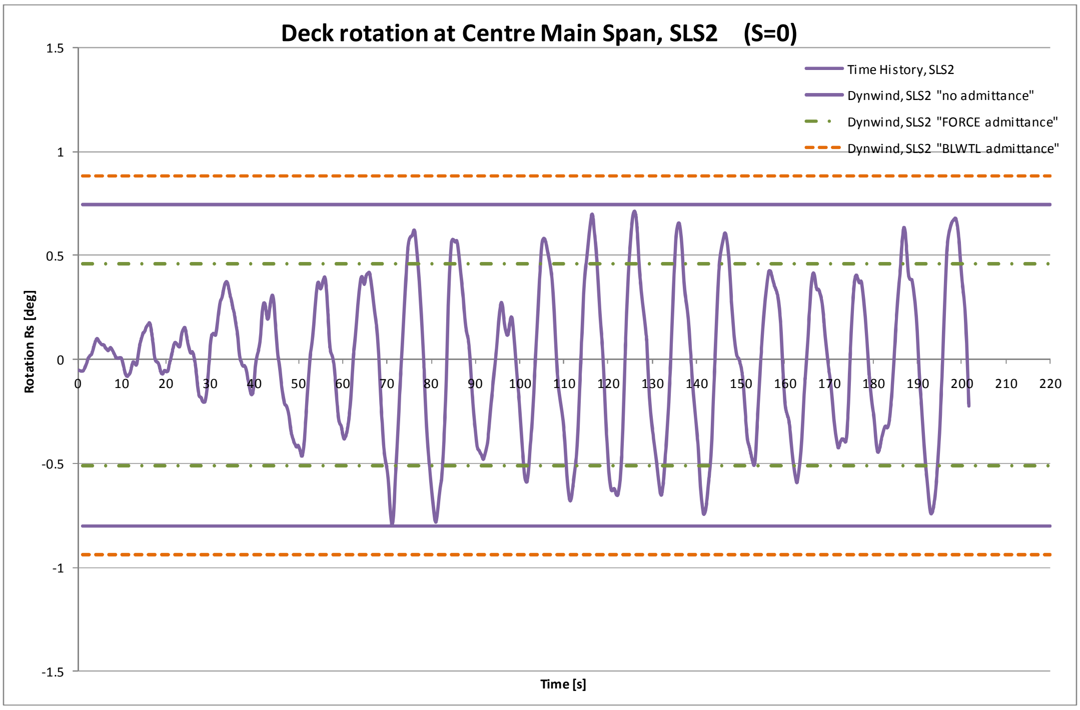


*Figure 5.16 Buffeting comparisons torsion response, SLS2.*

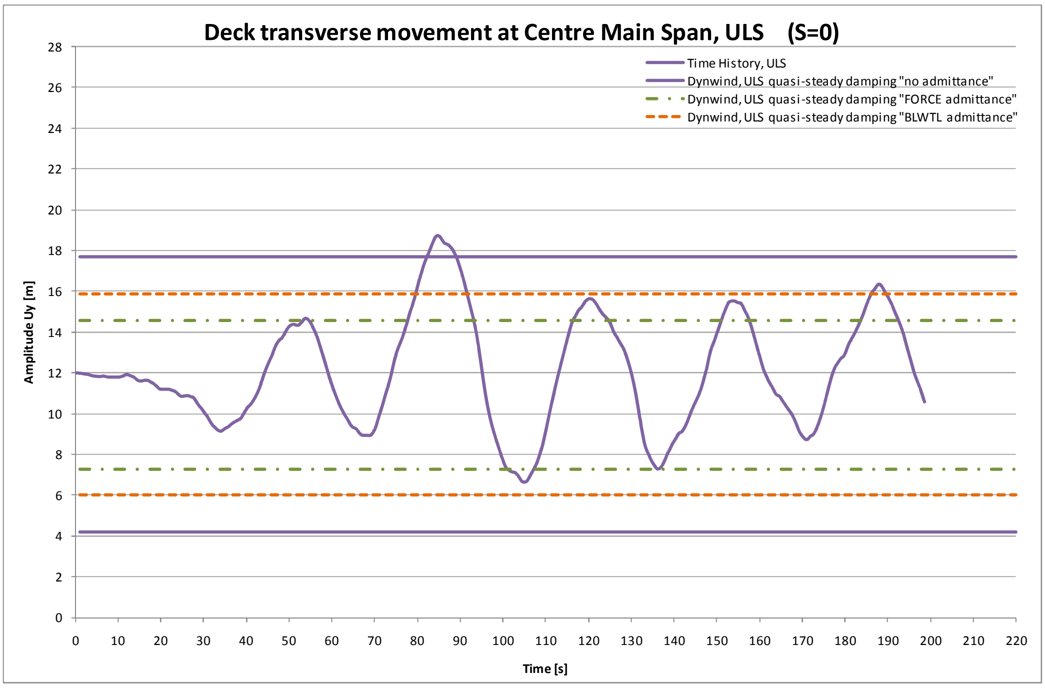


*Figure 5.17 Buffeting comparisons horizontal response, ULS.*

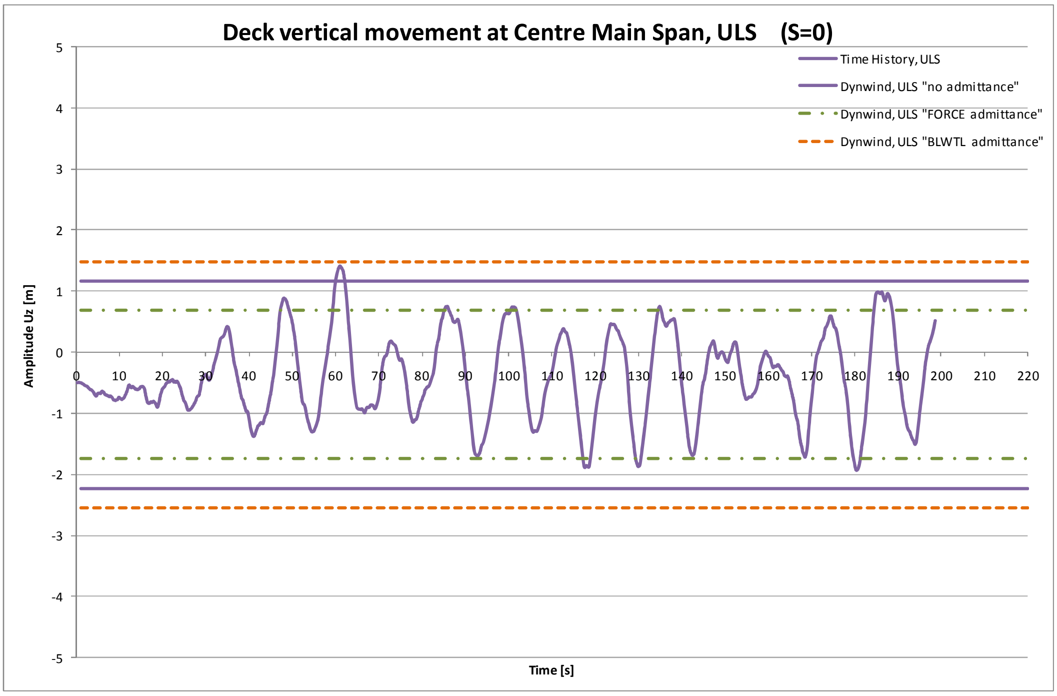


*Figure 5.18 Buffeting comparisons vertical response, ULS.*

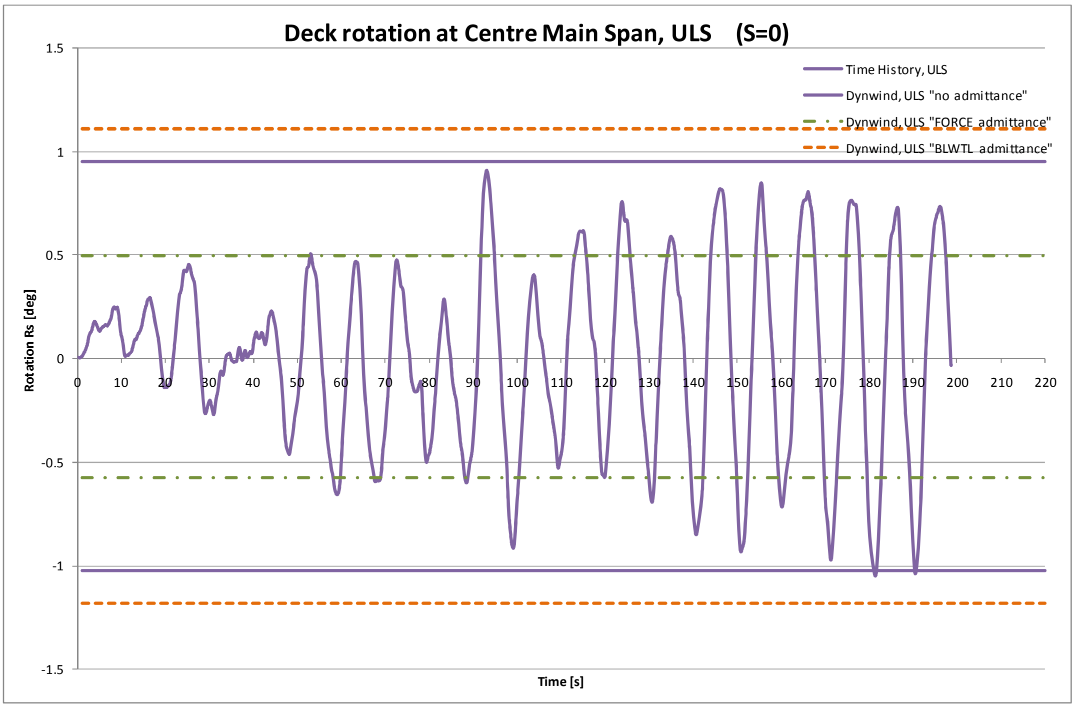


*Figure 5.19 Buffeting comparisons torsion response, ULS.*

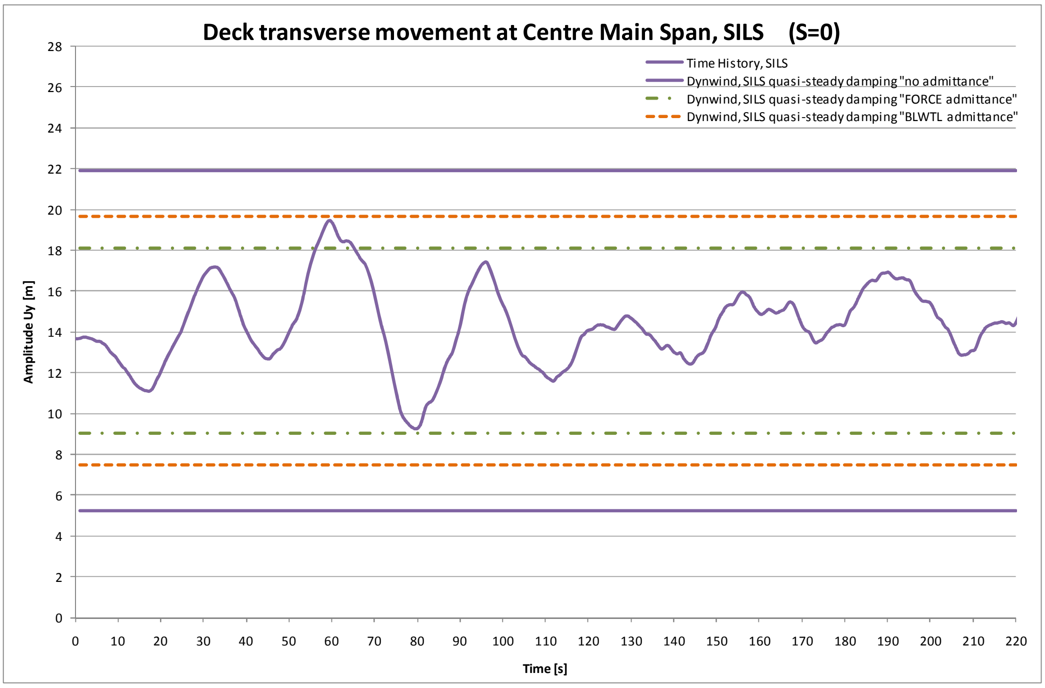


*Figure 5.20 Buffeting comparisons orizontal response, SILS*

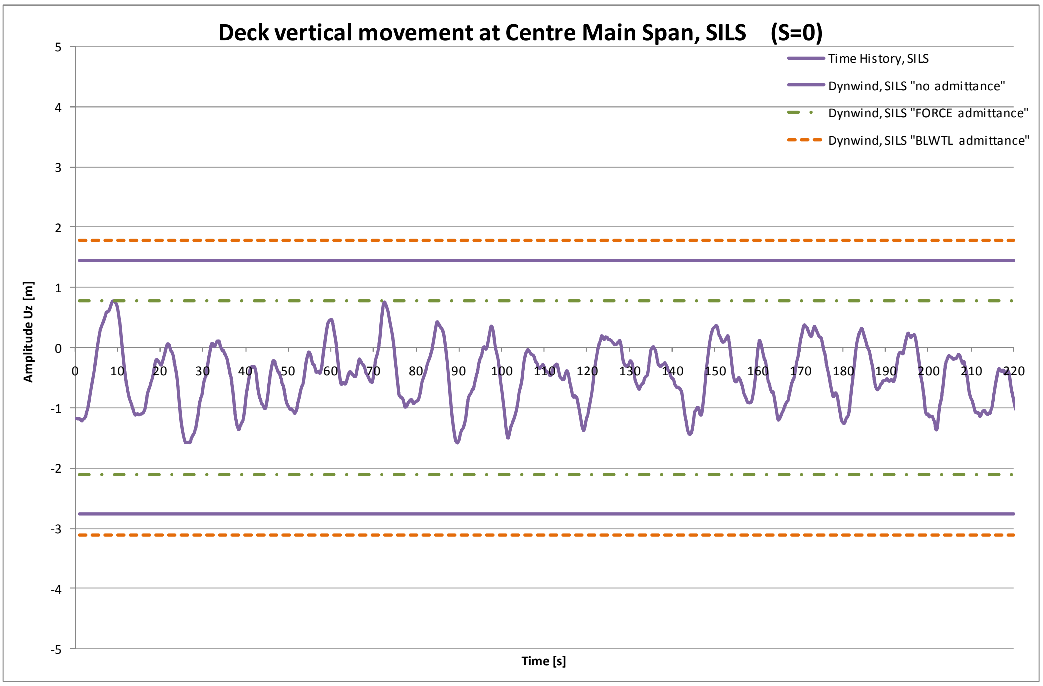


*Figure 5.21 Buffeting comparisons vertical response, SILS.*

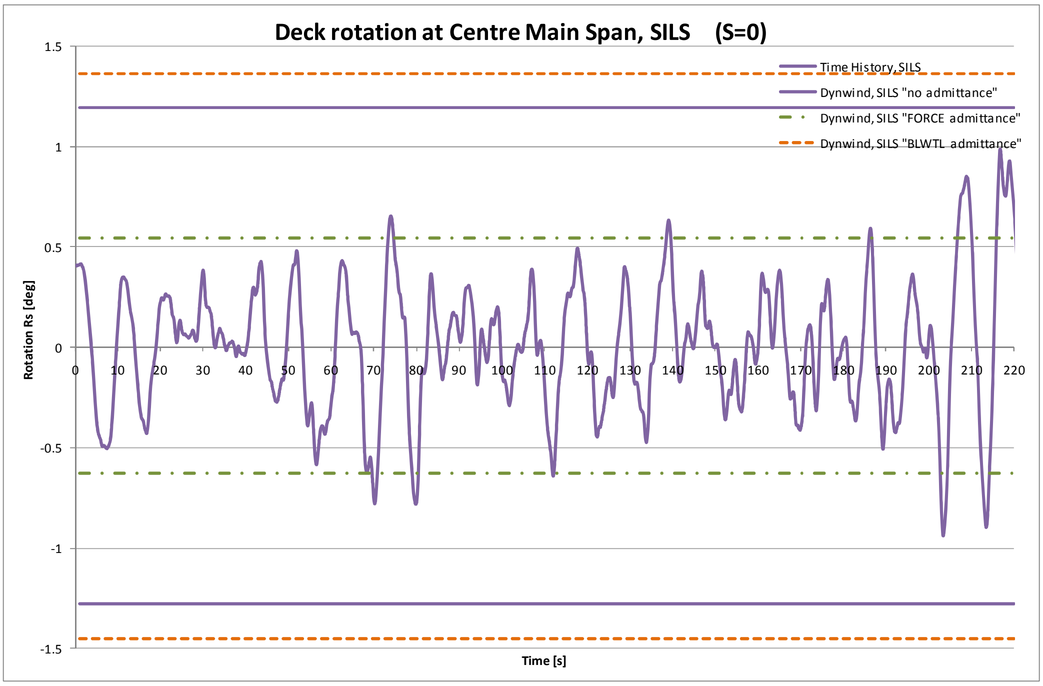


*Figure 5.22 Buffeting comparisons torsion response, SILS.*

### 5.5.1 Peak values for centre of the main span (S = 0)

*Table 5.2 Comparison of calculated horizontal peak responses at mid span.*

| **Time History** | Uy, max [m] | Uy, min [m] |
|---|---|---|
| SLS1 (44 m/s @ 70m) | 10.428 | 6.129 |
| SLS2 (47 m/s @ 70m) | 10.971 | 6.432 |
| ULS (54 m/s @ 70m) | 18.749 | 6.632 |
| SILS (60 m/s @ 70m) | 19.481 | 9.257 |

| **Dynwind (no adittance)** | Uy, max [m] | Uy, min [m] |
|---|---|---|
| SLS1 | 12.086 | 2.832 |
| SLS2 | 13.835 | 3.243 |
| ULS | 17.666 | 4.174 |
| SILS | 21.931 | 5.256 |

*Table 5.3 Comparison of calculated vertical peak responses at mid span.*

| **Time History** | Uz, max [m] | Uz, min [m] |
|---|---|---|
| SLS1 (44 m/s @ 70m) | 0.572 | -1.392 |
| SLS2 (47 m/s @ 70m) | 0.714 | -1.383 |
| ULS (54 m/s @ 70m) | 1.409 | -1.940 |
| SILS (60 m/s @ 70m) | 0.783 | -1.589 |

| **Dynwind (no adittance)** | Uz, max [m] | Uz, min [m] |
|---|---|---|
| SLS1 | 0.771 | -1.499 |
| SLS2 | 0.893 | -1.727 |
| ULS | 1.162 | -2.229 |
| SILS | 1.441 | -2.769 |

*Table 5.4 Comparison of calculated torsion peak responses at mid span.*

| **Time History** | Rs, max [deg] | Rs, min [deg] |
|---|---|---|
| SLS1 (44 m/s @ 70m) | 0.46 | -0.55 |
| SLS2 (47 m/s @ 70m) | 0.71 | -0.80 |
| ULS (54 m/s @ 70m) | 0.91 | -1.05 |
| SILS (60 m/s @ 70m) | 0.99 | -0.94 |

| **Dynwind (no adittance)** | Rs, max [deg] | Rs, min [deg] |
|---|---|---|
| SLS1 | 0.65 | -0.70 |
| SLS2 | 0.74 | -0.80 |
| ULS | 0.95 | -1.03 |
| SILS | 1.19 | -1.28 |

## 5.6 Deflection at ¼ point in the main span (S = -825)

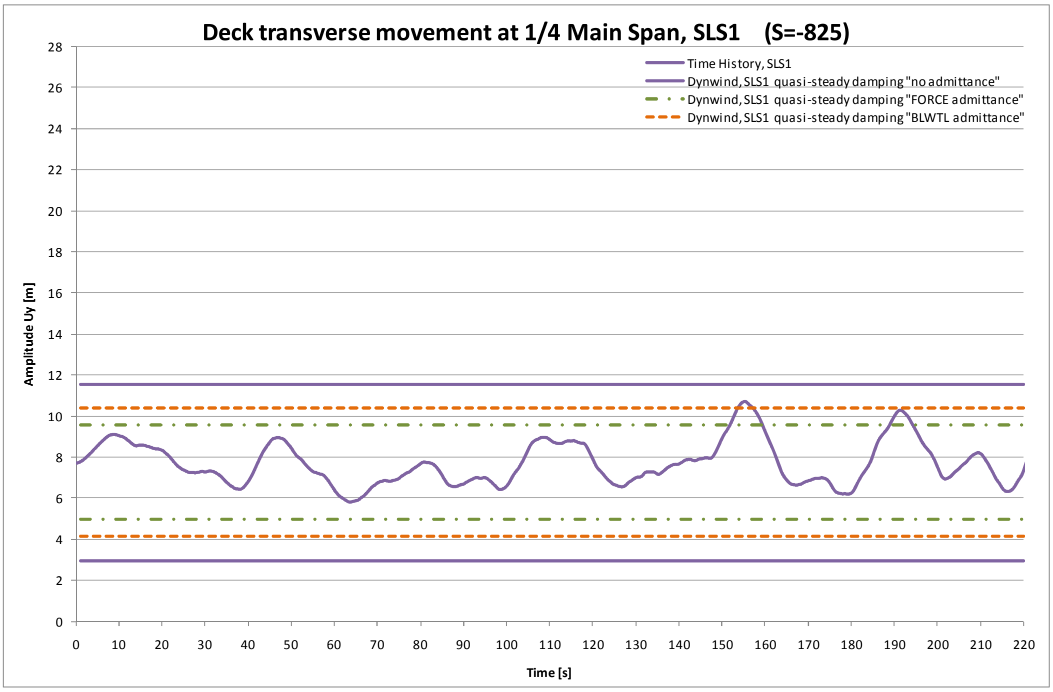


*Figure 5.23 Buffeting comparisons horsizontal response, SLS1.*

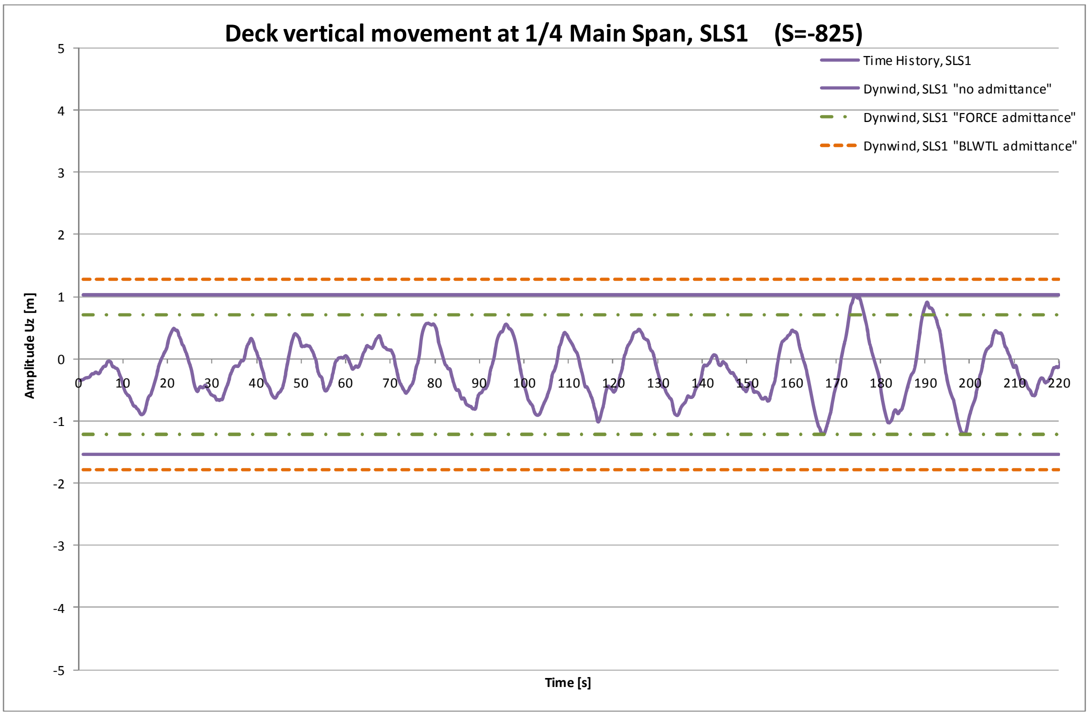


*Figure 5.24 Buffeting comparisons vertical response, SLS1.*

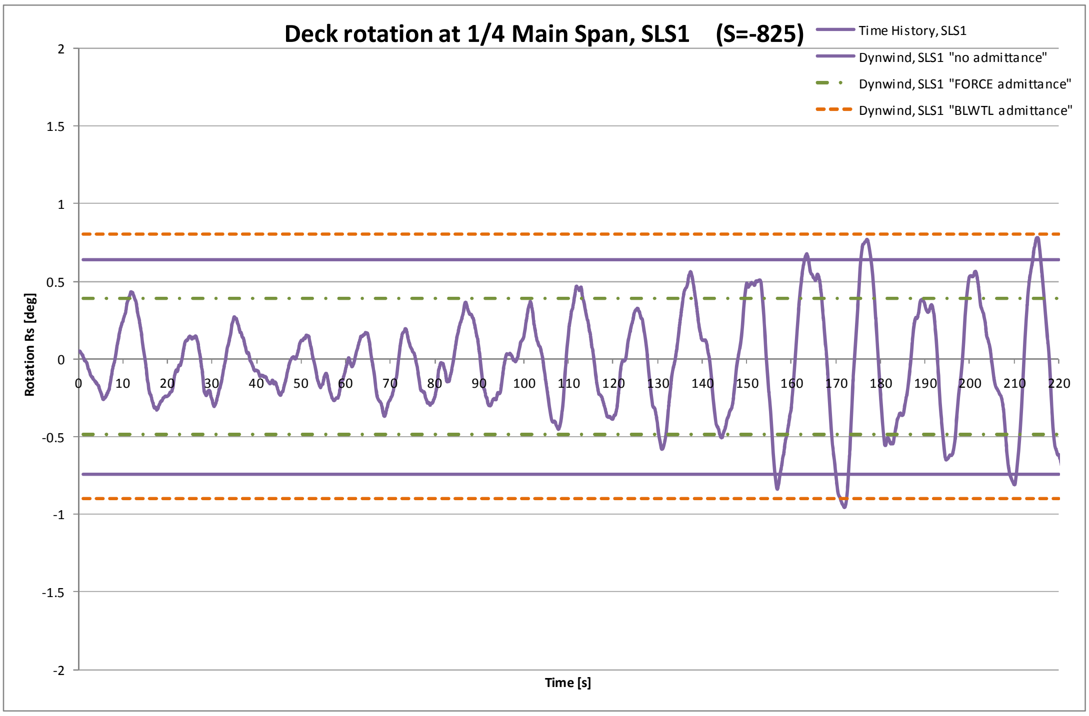


*Figure 5.25 Buffeting comparisons torsion response, SLS1.*

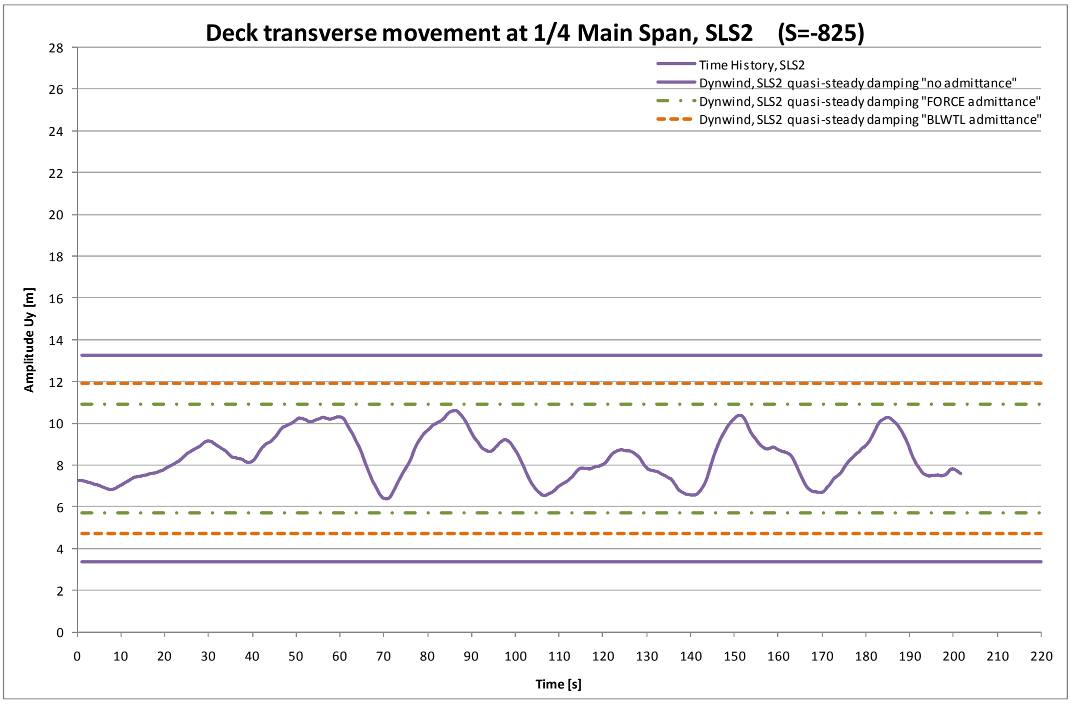


*Figure 5.26 Buffeting comparisons horizontal response, SLS2.*

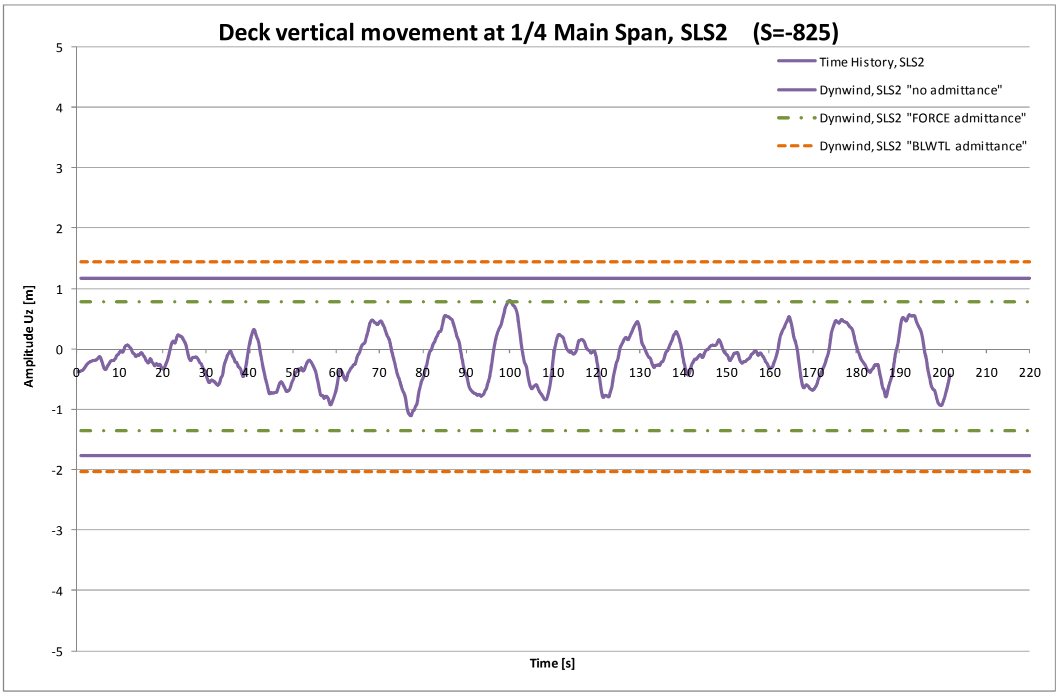


*Figure 5.27 Buffeting comparisons vertical response, SLS2.*

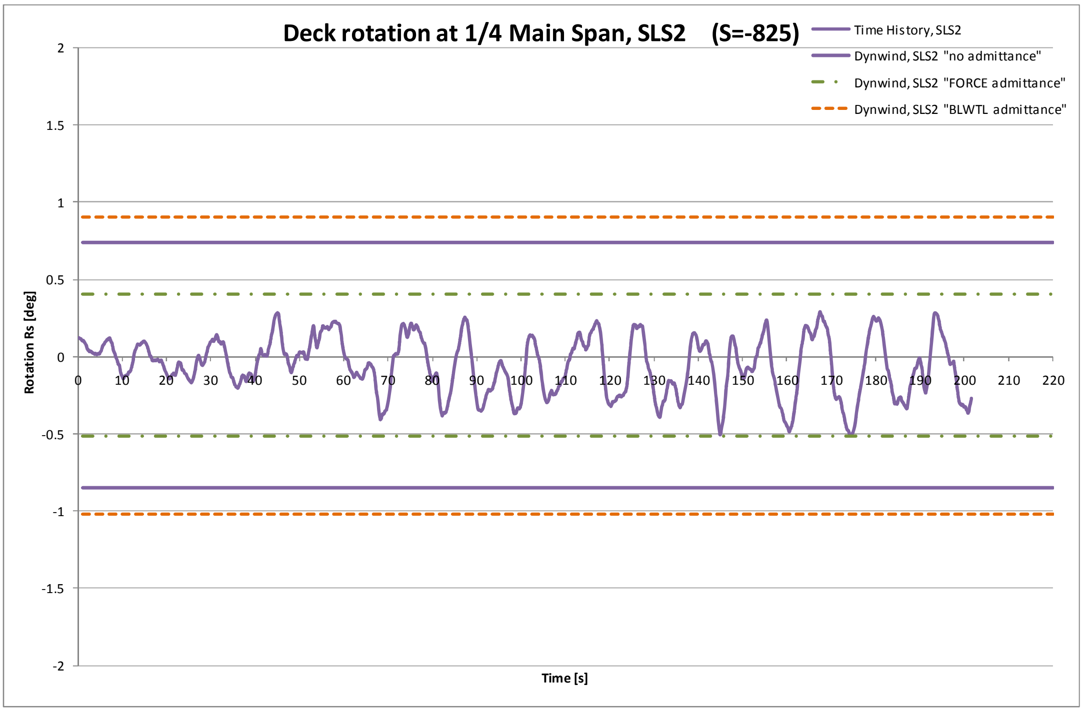


*Figure 5.28 Buffeting comparisons torsion response, SLS2.*

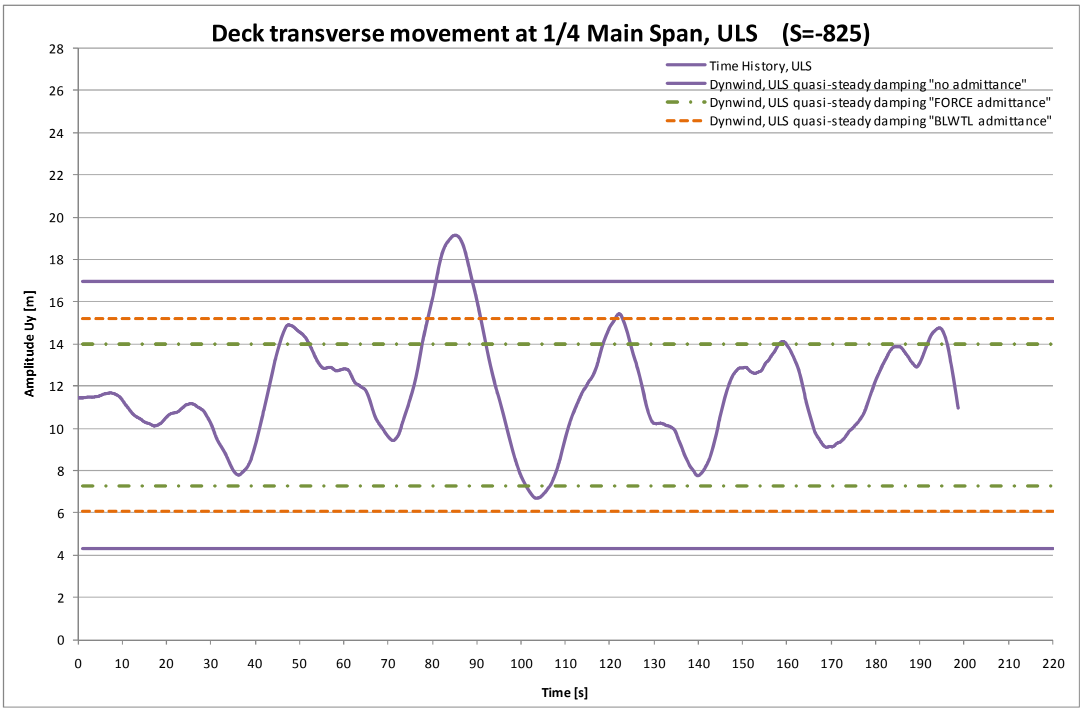


*Figure 5.29 Buffeting comparisons horizontal response, ULS.*

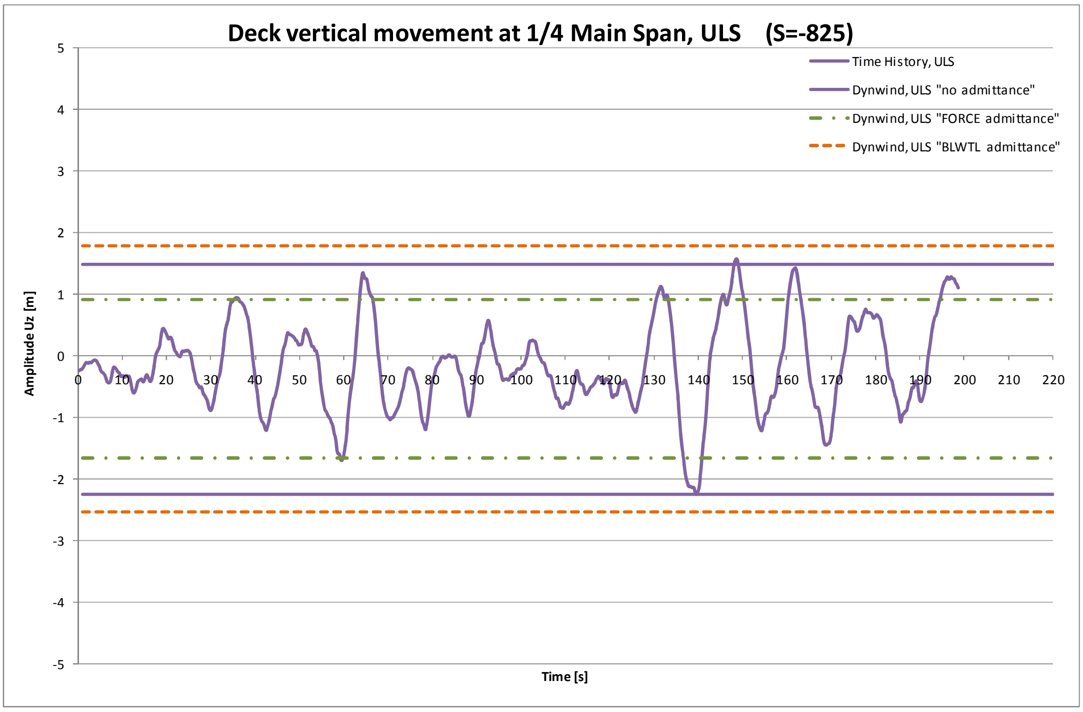


*Figure 5.30 Buffeting comparisonsvertical response, ULS.*

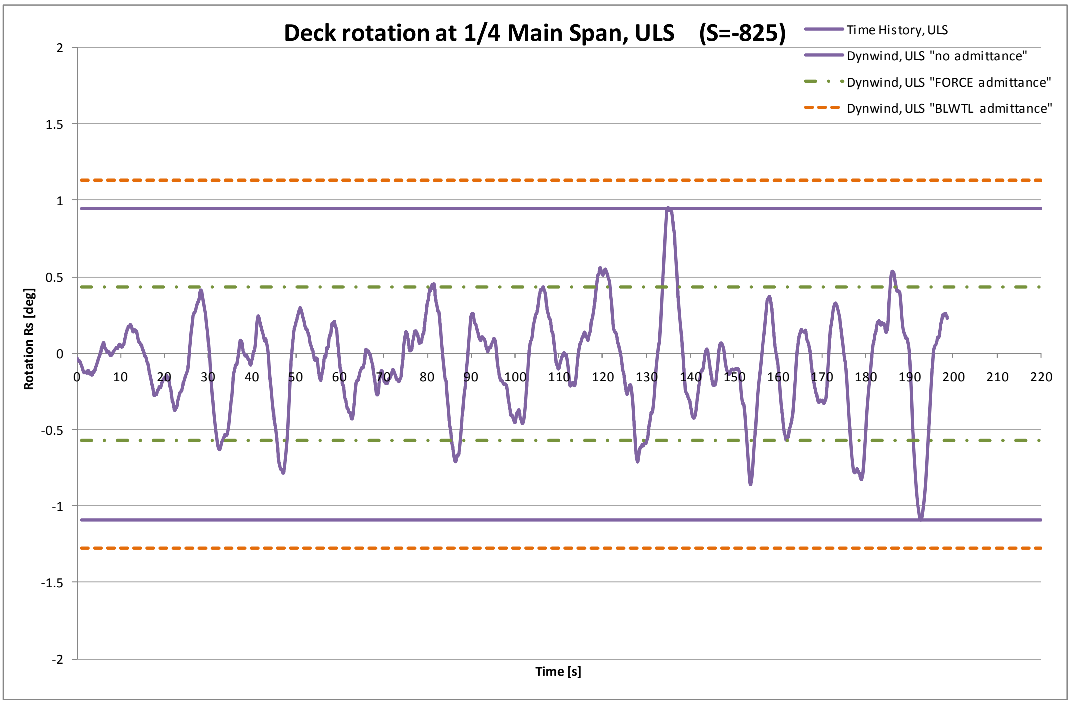


*Figure 5.31 Buffeting comparisons torsion response, ULS.*

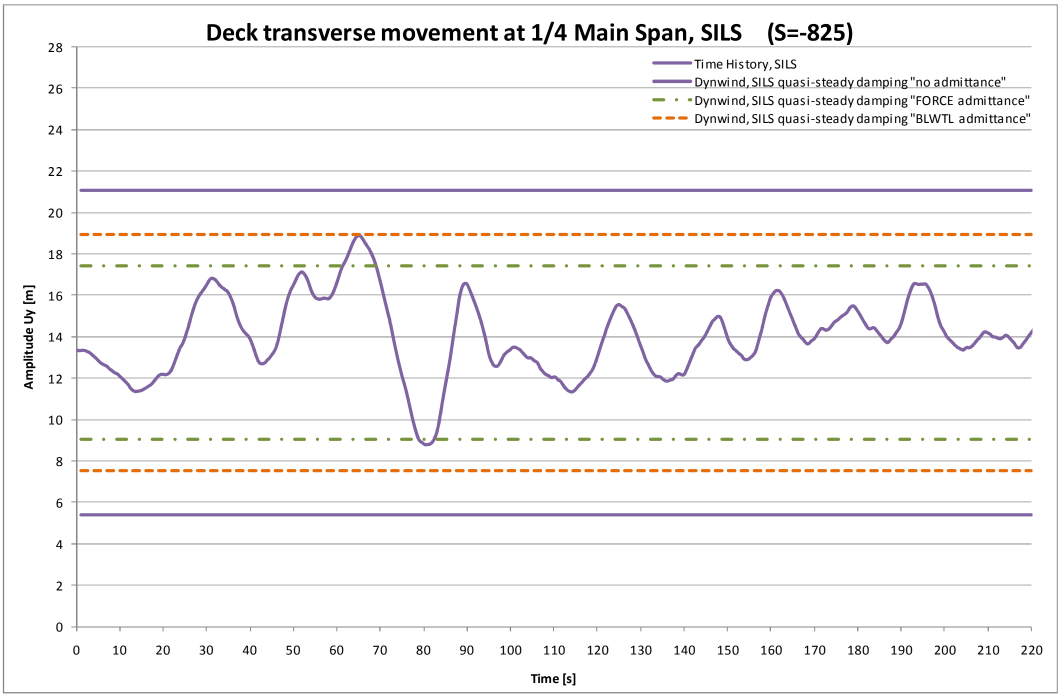


*Figure 5.32 Buffeting comparisons horizontal response, SILS.*

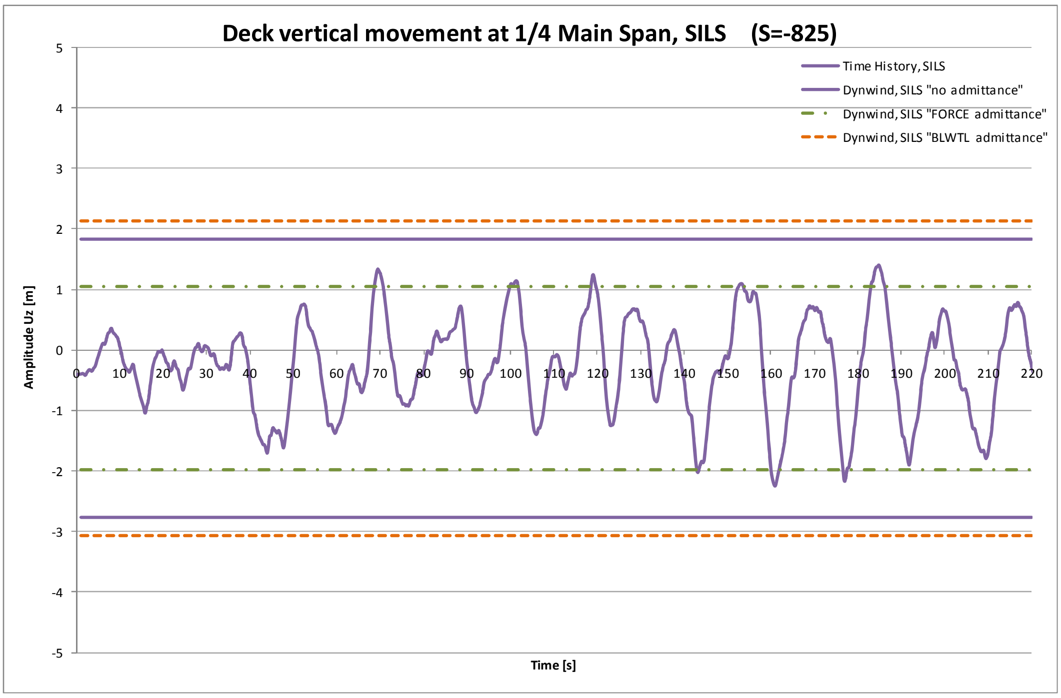


*Figure 5.33 Buffeting comparisonsvertical response, SILS.*

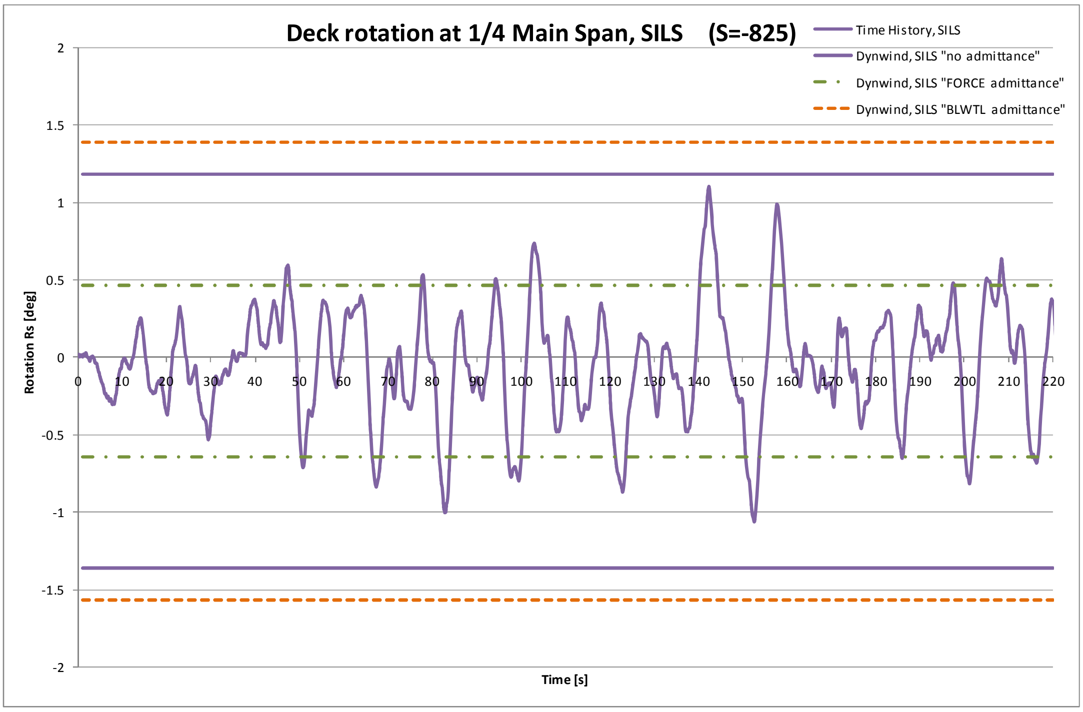


*Figure 5.34 Buffeting comparisons torsion response, SILS.*

### 5.6.1 Peak values for ¼ point in the main span

*Table 5.5 Comparison of calculated horizontal peak responses at quarter span.*

| **Time History** | Uy, max [m] | Uy, min [m] |
|---|---|---|
| SLS1 (44 m/s @ 70m) | 10.730 | 5.806 |
| SLS2 (47 m/s @ 70m) | 10.625 | 6.374 |
| ULS (54 m/s @ 70m) | 19.118 | 6.681 |
| SILS (60 m/s @ 70m) | 18.889 | 8.780 |

| **Dynwind (no adittance)** | Uy, max [m] | Uy, min [m] |
|---|---|---|
| SLS1 (44 m/s @ 70m) | 11.565 | 2.955 |
| SLS2 (47 m/s @ 70m) | 13.249 | 3.375 |
| ULS (54 m/s @ 70m) | 16.940 | 4.319 |
| SILS (60 m/s @ 70m) | 21.055 | 5.408 |

*Table 5.6 Comparison of calculated vertical peak responses at quarter span.*

| **Time History** | UZ, max [m] | UZ, min [m] |
|---|---|---|
| SLS1 (44 m/s @ 70m) | 1.011 | -1.210 |
| SLS2 (47 m/s @ 70m) | 0.789 | -1.110 |
| ULS (54 m/s @ 70m) | 1.576 | -2.251 |
| SILS (60 m/s @ 70m) | 1.407 | -2.244 |

| **Dynwind (no adittance)** | UZ, max [m] | UZ, min [m] |
|---|---|---|
| SLS1 (44 m/s @ 70m) | 1.022 | -1.535 |
| SLS2 (47 m/s @ 70m) | 1.171 | -1.758 |
| ULS (54 m/s @ 70m) | 1.490 | -2.241 |
| SILS (60 m/s @ 70m) | 1.835 | -2.770 |

*Table 5.7 Comparison of calculated torsion peak responses at quarter span.*

| **Time History** | Rs, max [deg] | Rs, min [deg] |
|---|---|---|
| SLS1 (44 m/s @ 70m) | 0.78 | -0.95 |
| SLS2 (47 m/s @ 70m) | 0.29 | -0.51 |
| ULS (54 m/s @ 70m) | 0.95 | -1.09 |
| SILS (60 m/s @ 70m) | 1.10 | -1.06 |

| **Dynwind (no adittance)** | Rs, max [rad] | Rs, min [rad] |
|---|---|---|
| SLS1 (44 m/s @ 70m) | 0.64 | -0.74 |
| SLS2 (47 m/s @ 70m) | 0.74 | -0.85 |
| ULS (54 m/s @ 70m) | 0.95 | -1.09 |
| SILS (60 m/s @ 70m) | 1.19 | -1.36 |

## 5.7 Deflection at tower top, Sicilia

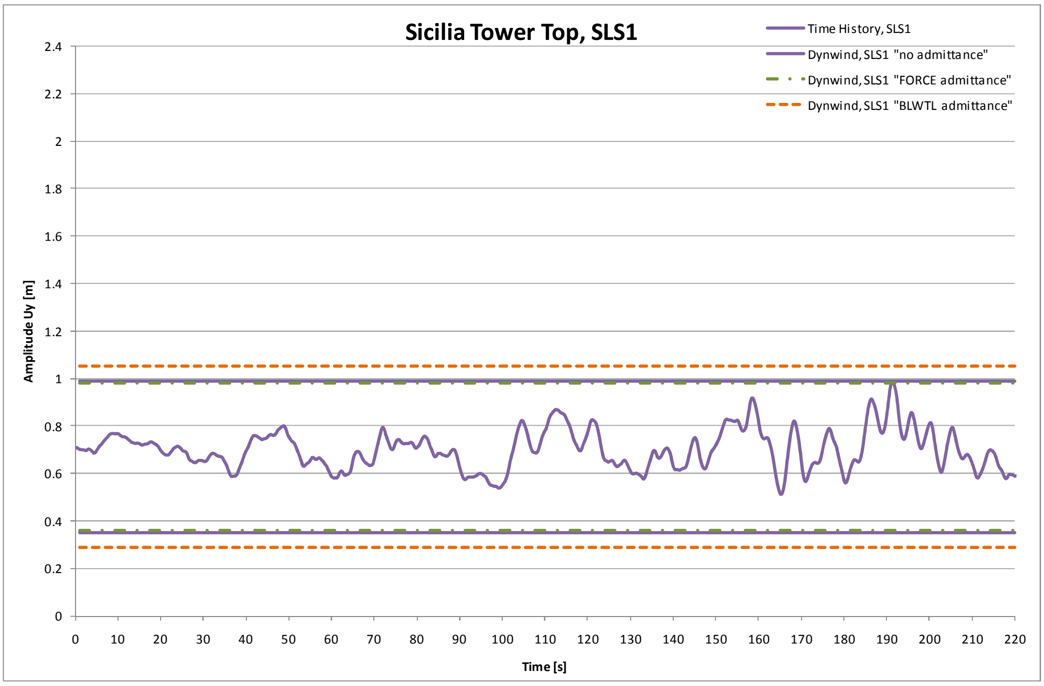


*Figure 5.35 Buffeting comparisons along wind response, SLS1.*

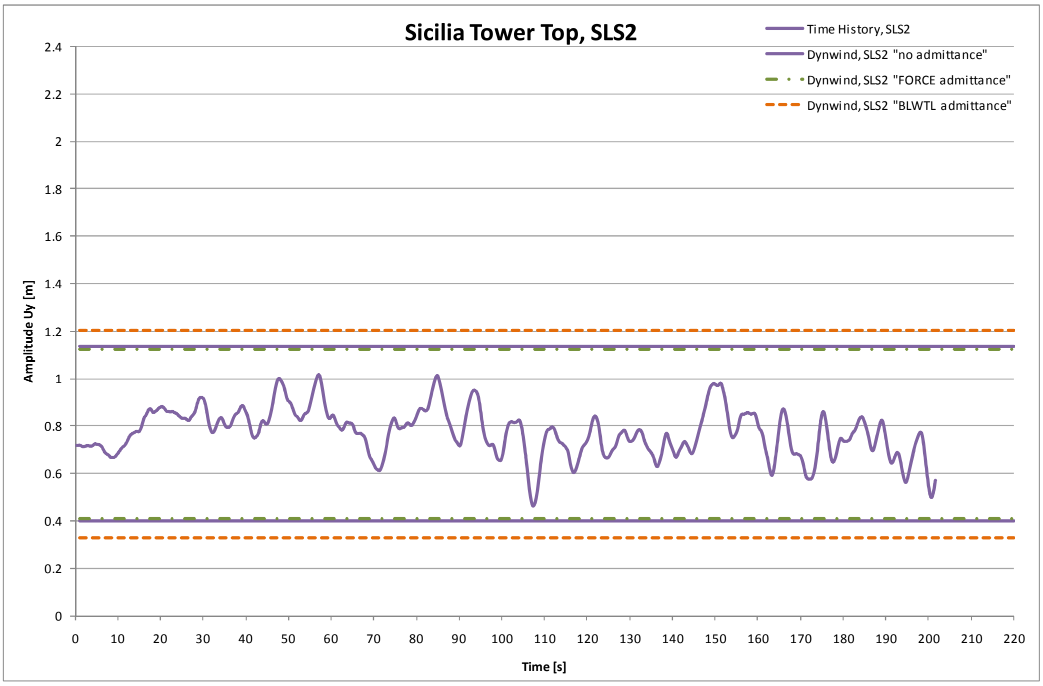


*Figure 5.36 Buffeting comparisons along wind response, SLS2.*

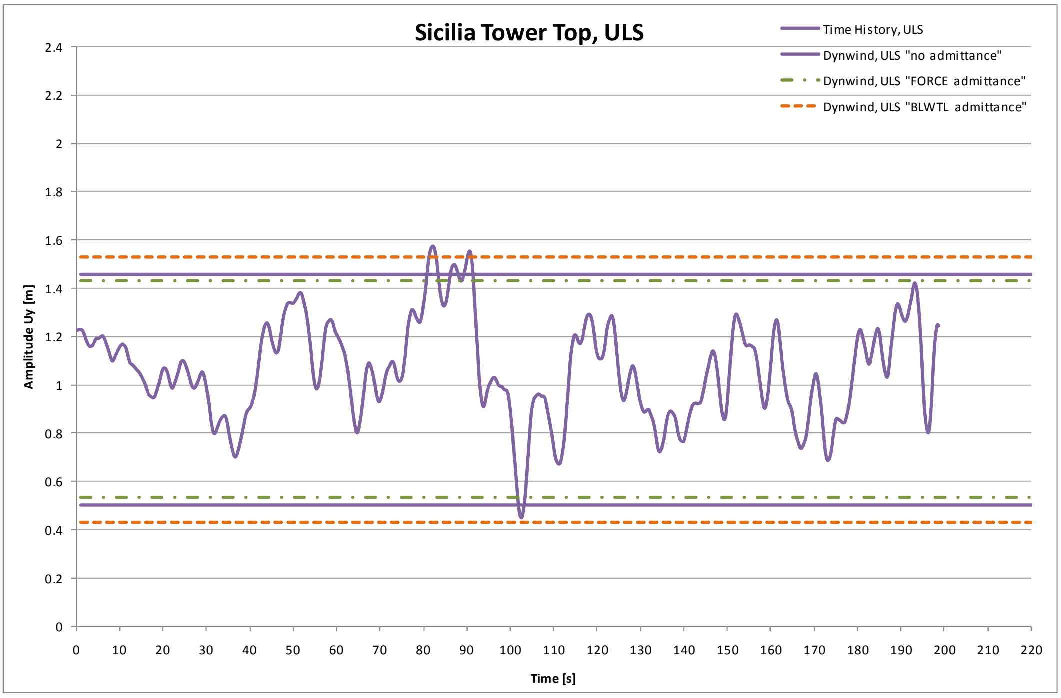


*Figure 5.37 Buffeting comparisons along wind response, ULS.*

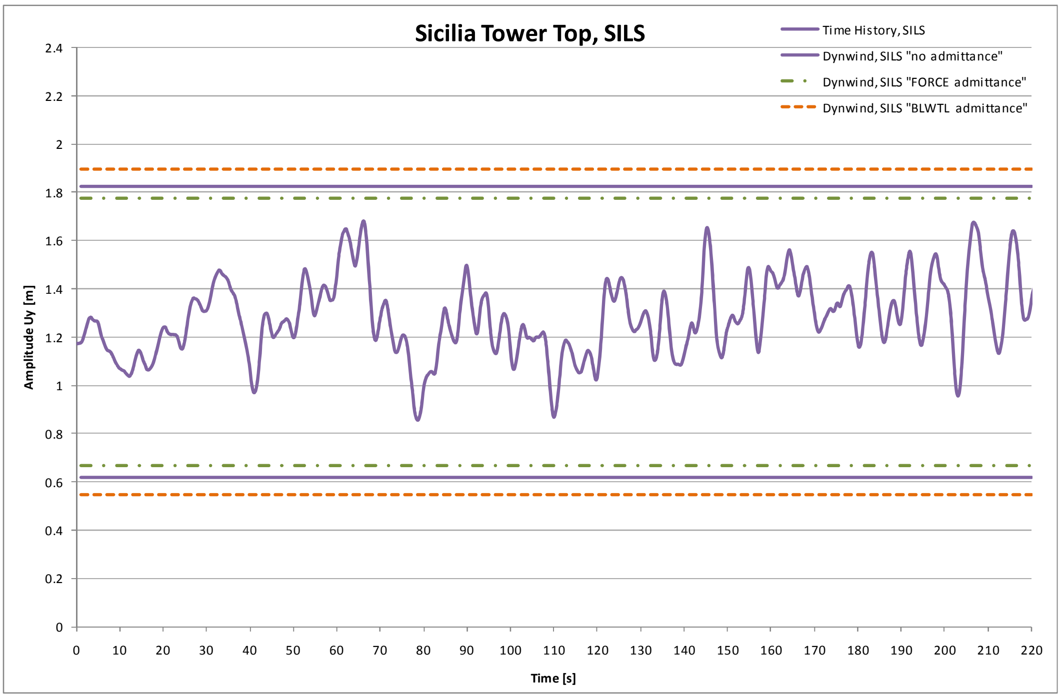


*Figure 5.38 Buffeting comparisons along wind response, SILS.*

### 5.7.1 Peak values for transverse movements in Sicilia tower top

*Table 5.8 Comparison of time and frequency domain along wind response.*

| **Time History** | Uy, max [m] | Uy, min [m] |
|---|---|---|
| SLS1 (44 m/s @ 70m) | 0.985 | 0.512 |
| SLS2 (47 m/s @ 70m) | 1.016 | 0.463 |
| ULS (54 m/s @ 70m) | 1.574 | 0.449 |
| SILS (60 m/s @ 70m) | 1.682 | 0.854 |

| **Dynwind (no adittance)** | Uy, max [m] | Uy, min [m] |
|---|---|---|
| SLS1 (44 m/s @ 70m) | 1.175 | 0.164 |
| SLS2 (47 m/s @ 70m) | 1.344 | 0.190 |
| ULS (54 m/s @ 70m) | 1.697 | 0.265 |
| SILS (60 m/s @ 70m) | 2.096 | 0.345 |

## 5.8 Discussion of the results

Generally the responses obtained from the time history analyses display fair agreement with frequency domain responses with frequency domain responses generally being highest. This is a reassuring finding as frequency domain analyses were used in the structural desing of the bridge.

The responses from the time history analyses show that the dominant modes of vibration are the $1^{st}$ and $2^{nd}$ transversal mode of the deck, i.e. approx 30sec and 20sec vibration period.

The response from ULS seem slightly higher than the response found from the other limit states, when compared to the dynamic wind analysis at short intervals, especially after approx 85 seconds into the analysis. The results show that the max response from ULS at the deck locations is comparable to the SILS response. This result may be explained by a prolonged high gust wind 70 seconds into the ULS time series, as shown in Figure 5.39. The same situation occurs near the end of the time series, with corresponding higher structural response.

Finally in comparing time domain and frequency domain analyses it should be remembered that at a given simulated wind time series constitutes only one realisation of the wind statistics at a given mean wind speed and also that the simulated wind time series of 3.5 min. length are short compared to the commonly appled statistical averaging period of 10 min. In order to obtain a more complete picture of the statistical variability, the structural response to several wind time series for the same mean wind speed should be simulated and compared.

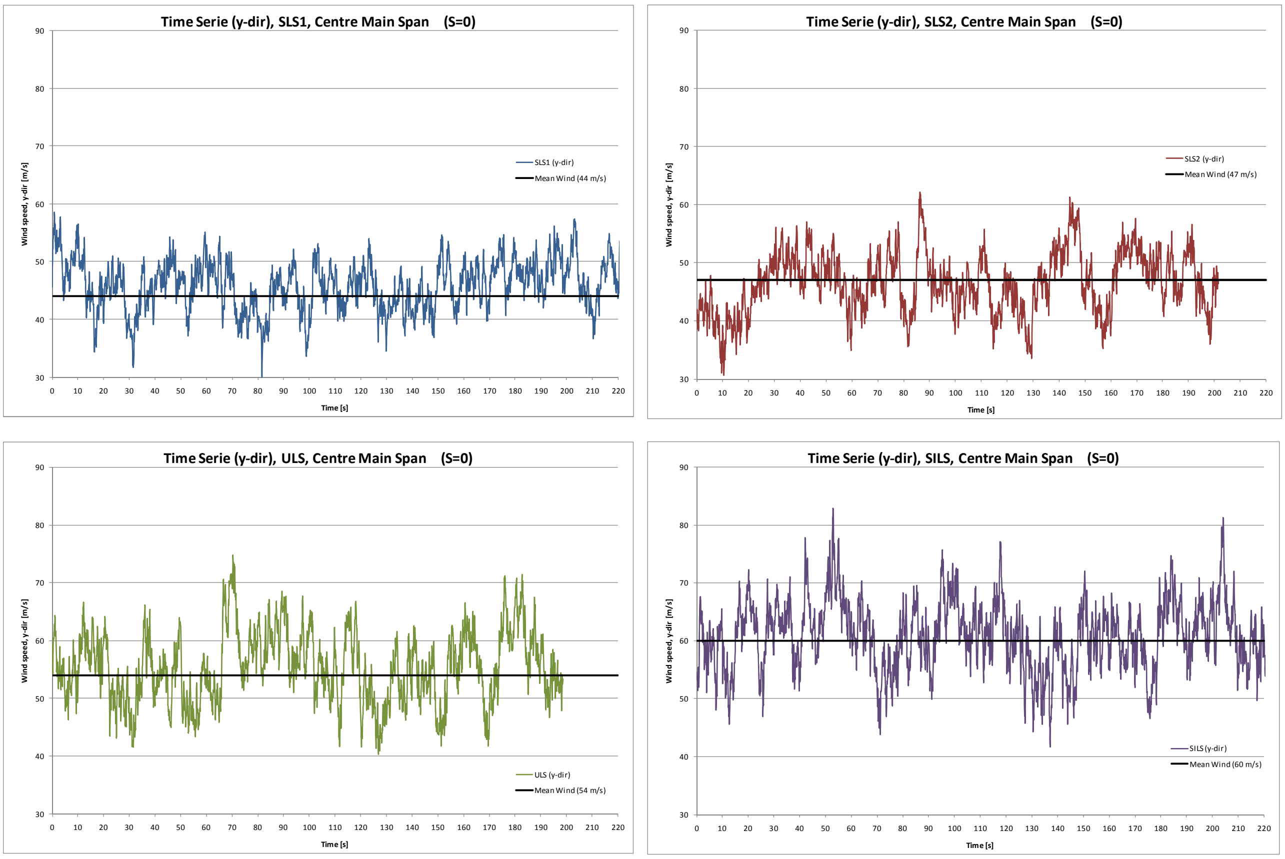


*Figure 5.39 Simulated wind speeds for the four load cases.*

The dynamic wind analyses carried out during design do not take admittance into account, which from the results is seen to be a conservative approach.

# 6 Future activities

Validation of the frequency and time domain buffeting computations have only been possible for the fundamental vertical and torsion modes as these are the only modes presented in the FORCE section model.

As the horizontal modes dominates the buffeting response and the design stresses in the bridge structure, it is proposed that further comparisons between buffeting computations and wind tunnel test are made during the Progetto Esecutivo phase when the results of the planned full bridge model tests becomes available.

# 7 References

1 EUROLINK S.C.p.A. CG1000-P-RG-D-P-SB-S3-00-00-00-00-02, Rev. B/ 2011-03-07, Wind Tunnel Tests, Girder. 2010.

2 EUROLINK S.C.p.A. CG1000-P-RG-D-P-SB-S3-00-00-00-00-01, Rev. B/ 2011-03-07, Wind Tunnel Tests, Towers. 2010.

3 EUROLINK S.C.p.A. CG1000-P-RG-D-P-SB-S3-00-00-00-00-03, Rev. B/ 2011-03-07, Wind Tunnel Tests, Cables. 2010.

4 BLWTL. A study of wind effects for the Messina Strait Bridge, Italy, deck section model - subtests D3 and D6. BLWTL-SS42-2010/Draft 4. January 2011.

5 Davenport, A.G.: The prediction of the response of structures to gusty wind. In safety of structures under dynamic loading, Tapir 1977.

6 FORCE: Sub-tests D4 Section Model tests for the Messina Strait Bridge. FORCE 110-26444 Rev.1 / 2011-03-01.

7 Stretto di Messina. Engineering - Definitive and Detailed Design, Basis of design and expected performance levels for the bridge (English translation). GCG.F.04.01. 2004-10-27.